Elsevier Editorial System(tm) for Journal of Chromatography A

Manuscript Draft

Manuscript Number: JCA-18-1284R2

Title: On the effect of chiral selector loading and mobile phase composition on adsorption properties of latest generation fully- and superficially-porous Whelk-O1 particles for high-efficient ultrafast enantioseparations

Article Type: Full length article

Keywords: Chiral Stationary Phases; Whelk-O1 selector; Superficially Porous Particles; Sub-2µm Fully Porous Particles; Adsorption Isotherms

Corresponding Author: Dr. Martina Catani, Ph.D.

Corresponding Author's Institution: University of Ferrara

First Author: Simona Felletti

Order of Authors: Simona Felletti; Chiara De Luca; Omar H Ismail, Ph.D.; Luisa Pasti, Ph.D.; Valentina Costa, Ph.D.; Francesco Gasparrini; Alberto Cavazzini, Ph.D.; Martina Catani, Ph.D.

Abstract: The adsorption isotherms of trans-stilbene oxide (TSO) enantiomers have been measured under a variety of normal phase (NP) mobile phases (MPs) on three Whelk-O1 chiral stationary phases (CSPs), prepared respectively on 1.8 µm and 2.5 µm fully porous particles (FPPs) and 2.6 µm superficially porous particles (SPPs). Specific loading of chiral selector (moles per square meter) of the two FPPs was about 20% smaller than that of SPPs (even if they were prepared under exactly the same experimental conditions).
Regardless of particle size or format, adsorption was described by means of a Bilangmuir model with ethanol/hexane MPs. On the other hand, in pure hexane, the Tóth isotherm was employed. Interestingly, it was found that selective and nonselective Henry's constants vary in opposite directions by increasing the percentage of strong MP modifier (between 3 and 10%, v/v). Saturation capacity of SPPs (referred only to the porous zone of the particle) was remarkably smaller than those of FPPs. On the other hand, binding constants on both selective and nonselective sites were significantly larger on SPPs. Finally, a correlation between the specific loading of chiral selector and the binding constants of enantiomers was suggested by data, which can be important also to understand the kinetic behavior of these particles in chiral ultrafast applications.

UNIVERSITY OF FERRARA
Department of Chemistry and
Pharmaceutical Sciences

Via L. Borsari 46, 44121 Ferrara, Italy
Fax:+39-0532-240709

Università degli Studi di Ferrara

Ref.: Revision MS JCA-18-1284R1

Dear Editor,

We are pleased to send you our revised version of MS **JCA-18-1284R1** according to reviewer's comment.

Attached as a separate file, you will find our response to the comment raised by reviewer #2 to **JCA-18-1284R1.** Our answer is reported in italic after reviewer's comment.

For your convenience, we also prepared a pdf version of the revised manuscript where changes have been tracked in red.

Thank you in advance for your time and cooperation.

With best regards,

Martina Catani

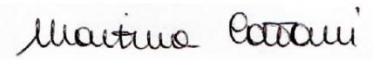

Reviewer #2

The authors have well and detailed responded to the reviewers' comments. They provided very reasonable explanations in the responding letter but they did not really clarify the easily misunderstood and unfortunate term "true" enantioselectivity from a semantic point of view. The experimentally observed enantioseparations always depends on the mobile phase conditions, the spatial neighborhood of the immobilized chiral selectors on the surface, in the present case on amorphous silica, the morphology of the surface and the pore structure, etc. This includes the conformation of the chiral selector moiety and its solvation which depends on the temperature.
It is fully agreed solid state NMR experiments could give additional informations in comparison to solution NMR with respect to the influence of the spatial neighborhood of the chiral selector and of the effect of the solvent and the solvation of all the selector and silica sites.

In summary, I still recommend to add to the text more explicitly what with the term "<alpha>-true" is actually meant and what is behind this expression. The calculated term stereoselective "<alpha>-true" is not true from a semantic point of view, but it describes more detailed the contribution of the stereoselective and non-stereoselective portfolio of "intermolecular" interactions taking place at the solvated and stereochemically modified silica surface with the chiral analytes.
It is agreed the chemically modified surface is indeed heterogeneous in terms of its morphology, chemical composition and its "solvation" status as factor of the mobile phase composition and temperature. I agree, porous silica of the SPP and FPP type will vary and thus also the morphology of the modified silica surface leading to different values of the "<alpha>-true" term.

The reader of this important paper needs to better understand why the same chiral selector chemically bound on FPP and SPP silica can lead to different binding constants expressed as <alpha>-apparent and <alpha>-true.

> *We thank the reviewer for this observation. Accordingly, we have added a deeper explanation of what the term "<alpha>-true" applied to chiral chromatography is actually meaning (see ll. 251-266 of the revised version of the MS).*

On the effect of chiral selector loading and mobile phase composition on adsorption properties of latest generation fully- and superficially-porous Whelk-O1 particles for high-efficient ultrafast enantioseparations

Simona Felletti[a], Chiara De Luca[a], Omar H. Ismail[b], Luisa Pasti[a], Valentina Costa[a], Francesco Gasparrini[b], Alberto Cavazzini[a,*], Martina Catani[a,]**

[a]Department of Chemistry and Pharmaceutical Sciences, University of Ferrara, via L. Borsari 46, 44121 Ferrara, Italy
[b]Department of Drug Chemistry and Technology, "Sapienza" University of Rome, P. le Aldo Moro 5, 00185, Rome, Italy

Abstract

The adsorption isotherms of *trans*-stilbene oxide (TSO) enantiomers have been measured under a variety of normal phase (NP) mobile phases (MPs) on three Whelk-O1 chiral stationary phases (CSPs), prepared respectively on 1.8 μm and 2.5 μm fully porous particles (FPPs) and 2.6 μm superficially porous particles (SPPs). Specific loading of chiral selector (moles per square meter) of the two FPPs was about 20% smaller than that of SPPs (even if they were prepared under exactly the same experimental conditions).
Regardless of particle size or format, adsorption was described by means of a Bilangmuir model with ethanol/hexane MPs. On the other hand, in pure hexane, the Tóth isotherm was employed. Interestingly, it was found that selective and nonselective Henry's constants vary in opposite directions by increasing the percentage of strong MP modifier (between 3 and 10%, v/v). Saturation capacity of SPPs (referred only to the porous zone of the particle) was remarkably smaller than those of FPPs. On the other hand, binding constants on both selective and nonselective sites were sig-

*Corresponding author
**Corresponding author
Email addresses: cvz@unife.it (Alberto Cavazzini), ctnmtn@unife.it (Martina Catani)

nificantly larger on SPPs. Finally, a correlation between the specific loading of chiral selector and the binding constants of enantiomers was suggested by data, which can be important also to understand the kinetic behavior of these particles in chiral ultrafast applications.

Keywords: Chiral Stationary Phases; Whelk-O1 selector; Superficially Porous Particles; Sub-2μm Fully Porous Particles; Adsorption Isotherms.

1. Introduction

The design and development of high efficient particles, either sub-2μm fully porous (FPPs) [1–3] or (second-generation) superficially porous (SPPs) ones [4–12], functionalized with chiral selectors, have represented the most important innovation in the last decade in the field of chiral separations by liquid chromatography. Not only have they allowed for the preparation of packed columns with extraordinary kinetic performance – altogether comparable to that of typical reversed-phase (RP) achiral separations [13–15]– but they also have permitted to decrease the analysis time by up to three orders of magnitude (from tenths of minutes to fractions of seconds) [1–5, 12–14, 16–20].

Many remarkable examples showing the very large potential of new generation particles towards high-efficient ultrafast (sub-seconds) enantioseparations have been published [1–12]. Essentially, in all of these studies the key has been to use very short prototype columns (either 10 or even 5 mm long) operated at the maximum flow rate allowed by the equipment (between 5 and 8 mL/min depending on the brand of the instrument). At very large flow rates, the so-called mass transfer term, or *c*-term, of the van Deemter equation dominates over the other mechanisms of band broadening (longitudinal diffusion and eddy dispersion). Differently from what happens in RP achiral chromatography, in chiral chromatography this term accounts not only for diffusion of molecules through the particles of the packed bed (where flow is absent) but also for the adsorption-desorption kinetics. Adsorption-desorption kinetics is negligible in RP achiral chromatography unless very large molecules (such as proteins or large polypeptides) are considered. It has been indeed demonstrated that for small molecules adsorption-desorption is very fast ([21, 22]). On the opposite, the enantiorecognition process can be slow, even if the extent largely depends on the type of chiral selector employed. For instance, it is generally accepted that brush-type chiral selectors, such as the Whelk-O1 type, are "fast" while other kinds of selectors, including macrocyclic glycopeptides and polysaccharides, are "slow". This information basi-

cally comes from molecular spectroscopic investigation (firstly, by NMR). Therefore, it is not unusual that experimental conditions under which it was obtained can be significantly different from those typical of liquid chromatography. Not just because spectroscopic measurements are (very often) performed in homogeneous systems, where both chiral selectors and anaytes are in solution, but also since solvents employed in these measurements can be very different from typical eluents used in liquid chromatography. Thus, these measurements does not account for the effect of several variables that may affect chiral recognition in heterogenous systems (i.e., when the chiral selector is tethered to the surface), such as the chemical composition of the surface around chiral selector, the surface density of chiral selector, pore size and morphology, their accessibility, the competitive effect for adsorption by so-called strong mobile phase (MP) modifiers, etc.

For the reasons explained above, however, these considerations assume great importance for latest generation sub-2μm fully porous and second-generation superficially porous particles. This is particularly so when one wants to compare superficially- and fully-porous particles (functionalized with the same chiral selector) in terms of kinetic perfomance. The common reasoning [8, 23–27] about the alleged superiority, in terms of efficiency, of the former type of particles over their fully porous counterpart is based on the same considerations employed in achiral RP chromatography, namely that eddy dispersion, longitudinal diffusion and solid-liquid mass transfer are smaller on chiral SPPs than on FPPs. Therefore, these conclusions either completely neglect the role of adsorption-desorption kinetics or they implicitly assume that adsorption-desorption kinetics is identical on both kinds of particles. On the other hand, many authors report that functionalization of SPPs and FPPs systematically leads to different specific loading, or density (μmol/m^2) of chiral selectors on the two types of particles, even if their chemical modification is performed under exactly the same experimental conditions [1, 5, 8, 11, 13].

With the purpose of shedding light on some of these aspects, in this work the adsorption isotherms of *trans*-stilbene oxide (TSO) enantiomers have been measured under normal phase (NP) conditions on three different Whelk-O1 chiral stationary phases (CSPs). Two of them were prepared on FPPs (2.5 and 1.8 μm particle diameter, respectively) and the other one on 2.6 μm SPPs [1, 13]. The investigation of adsorption isotherms is fundamental not only to characterize surface heterogeneity (in terms of adsorption energy distribution) but also to investigate if, e.g., the bonding density has an effect on the binding constants of enantiomers and enantioselectivity of CSPs. In addition, since adsorption-desorption kinetics

is strongly influenced by thermodynamic equilibria [28], this information can also be useful to understand the chromatographic behavior of fully- and superficially-porous particles at high flow rates [1, 2, 29–31].

2. Theory

The equilibrium-dispersive (ED) model has often been used to describe chromatographic separations characterized by efficient mass transfer [28]. In this model, instantaneous equilibrium between mobile (MP) and stationary phase (SP) is assumed. Since both thermodynamics of phase equilibria and mass transfer kinetics change with experimental conditions, the only parameter that is conserved during a chromatographic separation (in absence of chemical reaction) is the mass of the injected sample. Therefore, a differential mass balance equation can be written that, for the ED model, includes an apparent lumped dispersion term (D_a) accounting for all the contributions to band broadening observed in linear chromatography:

$$\frac{\partial C_i}{\partial t} + F\frac{\partial q_i}{\partial t} + u\frac{\partial C_i}{\partial z} = D_{a,i}\frac{\partial^2 C_i}{\partial z^2} \tag{1}$$

where the index i indicates ith component of the system. In this equation, C_i and q_i are the concentrations of analyte in MP and SP, respectively, t represents the temporal coordinate and z the spatial one. Finally, u is the MP linear velocity and F the phase ratio:

$$F = \frac{1-\epsilon_t}{\epsilon_t} \tag{2}$$

being ϵ_t the total porosity of the packed bed given by the ratio between the hold-up, V_0, and the geometric volume, V_{col}, of the column. The apparent dispersion coefficient is calculated through the efficiency of the chromatographic peak under analytical conditions:

$$D_{a,i} = \frac{uL}{2N_i} \tag{3}$$

where N is the number of theoretical plates and L the column length. In the case of enantiomeric separations ($i = 1, 2$), the system will be described by two partial differential equations, which are coupled through a competitive isotherm equation, $q_i = f(C_1, C_2)$ (see later on).

2.1. Inverse Method for determination of isotherms

The direct numerical resolution of the system of mass balance equations requires the knowledge of the isotherm. This can be, for instance, evaluated through (competitive) frontal analysis. Contrary, in the so-called Inverse Method (IM) [32–34], isotherm parameters are derived through a procedure based on the iterative resolution of system of mass balance equations (once an isotherm model has been chosen). Isotherm parameters are calculated by minimizing the differences between experimental and calculated chromatograms. Schematically, IM requires the following steps: i) recording of some experimental overloaded profiles; ii) selection of an isotherm model (the shape of overloaded profiles guides this process [28]) and guess of initial parameters; iii) resolution of system of mass balance equations with the adsorption isotherm just selected (to get a calculated chromatogram); iv) comparison between calculated overloaded profiles and experimental ones; v) tuning of isotherm parameters until calculated and experimental profiles match as much as possible. Numerical optimization of isotherm parameters was made by means of the super-modified simplex method described in [32, 35].

To solve the system of mass balance equations, obviously proper initial and boundary conditions must be defined. In this work, the following initial

$$C_i(z, t = 0) = 0 \quad i = 1, 2 \tag{4}$$

and boundary

$$C_i(z = 0, t) = \begin{cases} C_{i,0} & 0 \leq t \leq t_{inj} \quad i = 1, 2 \\ 0 & t > t_{inj} \end{cases} \tag{5}$$

conditions were taken describing, respectively, that at $t = 0$ the column is equilibrated with pure eluent (Eq. 4) and that the injection profile is a rectangular pulse of concentration $C_{i,0}$ ($i = 1, 2$) during the injection time, t_{inj} (Eq. 5).

2.2. Isotherm models

2.2.1. Langmuir isotherm

The Langmuir model is the most frequently used to describe adsorption in liquid chromatography. Based on the Langmuir model, the adsorption surface is assumed to be paved by only one type of adsorption sites (homogeneous adsorption). In addition, adsorption is monolayer and no lateral interactions between adsorbed molecules are possible. In the case the

Langmuir isotherm is used to model chiral separations, not only it is assumed that nonselective interactions have a negligible contribution to retention of enantiomers but also that energies of all possible enantioselective interactions are close enough that they can be averaged. Accordingly, a single adsorption energy and a single adsorption constant can be defined, which characterize all adsorption sites on the surface. (Obviously, average energies and constants are different for the two enantiomers). The competitive Langmuir model applied to the separation of two enantiomers (denoted hereafter 1 and 2) is written as:

$$q_i = \frac{q_s b_i c_i}{1 + b_1 c_1 + b_2 c_2} \qquad i = 1, 2 \tag{6}$$

where q_s is the saturation capacity (equal for both enantiomers [28]) and b_i is the adsorption equilibrium (binding) constant. The product between q_s and b_i defines the so-called Henry's constant of adsorption, a_i (that is the initial slope of the isotherm). Retention factor (under linear condition), k, and Henry's constant are connected by:

$$k = \frac{t_R - t_0}{t_0} = aF \tag{7}$$

where t_R and t_0 are respectively the retention and hold-up time measured under linear conditions.

2.2.2. Tóth isotherm

This isotherm describes heterogeneous adsorption. In particular, it assumes a continuous and possibly wide adsorption energy distribution. Width depends on the value of the so-called heterogeneity parameter, ν ($0 < \nu < 1$). The smaller ν the wider the adsorption energy distribution function. For binary competitive systems, the Tóth isotherm is:

$$q_i = \frac{q_s b_i c_i}{[1 + (b_1 c_1 + b_2 c_2)^\nu]^{1/\nu}} \qquad i = 1, 2 \tag{8}$$

2.2.3. Bilangmuir isotherm

The Bilangmuir model, finally, accounts for a bimodal adsorption energy distribution due to the presence of two different adsorption sites that, in case of chiral separations, are considered selective (responsible for diastereomeric or enantioselective interactions) and nonselective (where both enantiomers behave identically) [36]. This model has been often successfully applied to describe adsorption processes of enantiomers on CSPs

[32, 37, 38]. The competitive 2-component adsorption isotherm is:

$$q_i = \frac{q_{sel} b_{i,sel} c_i}{1 + b_{1,sel} c_1 + b_{2,sel} c_2} + \frac{q_{nsel} b_{nsel} c_i}{1 + b_{nsel}(c_1 + c_2)} \qquad i = 1, 2 \tag{9}$$

where subscripts *sel* and *nsel* refer to selective and nonselective sites, respectively [28, 32, 39, 40].

3. Materials and methods

3.1. Columns and materials

All solvents and reagents were purchased from Sigma Aldrich (St. Louis, MI, USA). Kromasil fully porous silica particles (2.5 and 1.8 μm particle size, 100 Å pore size, 323 m^2/g specific surface area) were from Akzo-Nobel (Bohus, Sweden). Accucore second-generation superficially porous silica particles (2.6 μm, 80 Å pore size, 130 m^2/g specific surface area, radius of core over particle radius, $\rho = 0.63$) were from Thermo Fisher Scientific (Waltham, MA, USA). Whelk-O1 selector was generously donated by Regis Technologies Inc. (Morton Grove, IL, USA). Synthesis and preparation of Whelk-O1 CSPs are reported in Ref. [1]. 100 and 150 mm$\times$4.6 mm empty stainless steel columns were from IsoBar Systems by Idex (Erlangen, Germany).

3.2. Equipment

All measurements were performed on an Agilent 1100 Series Capillary LC system equipped with a binary solvent pump, a column thermostat and a photodiode array detector. An external manual injector (Rheodyne 8125, equipped with either 5 or 50 μL fixed-loops) was used for sample injections. Detector calibration was performed by sequentially injecting 50 μL TSO racemic solutions (concentration from 0.05 g/l to 5 g/L) without the column. This volume was large enouth to observe concentration plateau. Wavelength: 280 nm.

3.3. Experimental conditions

Adsorption isotherms were measured at five different hexane/ethanol MP compositions: 90/10, 92/8, 95/5, 97/3 and 100/0, % v/v. Temperature was 35°C. TSO racemic mixture injected concentrations were: 3, 10, 20, 40, 50 g/L. Injection volume was 5 μL.

4. Results and discussion

Table 1 reports some of the physico-chemical characteristics of particles and columns employed in this work [1, 2, 30]. Fully porous particles were used to prepare the columns named FPP-1.8 and FPP-2.5; the column called SPP-2.6 was packed with core-shell particles (see Table 1). Information on particle diameter, specific surface area and pore size comes from manufacturers. Bonding density was determined through elemental analysis (more information under SI). As expected, bonding densities per gram of base silica are larger on FPPs (for which essentially the same value was obtained regardless of particle size) than on SPPs. On the other hand, specific bonding density (μmol/m^2) is significantly larger (by almost 20%) on SPPs than that of FPPs. This last finding has been observed also with other chiral selectors [13] and by other authors [5, 8]. However, in other cases [7] the opposite was reported so that no generalization can be made. It is worth noting that functionalization of both SPPs and FPPs was performed under identical experimental conditions (and repeated several times). Nevertheless, specific bonding density was different. Among the hypotheses that can be formulated to explain why this happens, the different reactivity of surface silanol groups on the two kinds of particles or the different accessibility of intraparticle space (during particle functionalization) are the most likely. Particle porosity, ϵ_p, was measured as reported under SI. ϵ_p, describing the fraction of empty pores per particle, is consistent with values of specific bonding density.

To investigate whether the different specific bonding density of chiral selector entails changes on the CSPs, the adsorption isotherms of the enantiomers of a probe compound, TSO, were measured under NP conditions. Measuring the isotherms is the only approach to characterize the surface in terms of adsorption sites and their abundance. This information, on the other hand, cannot be gathered through measurements performed under linear conditions (i.e., by means of retention factors) [28, 32, 41–45].

Isotherms were measured through IM. Different competitive adsorption models were considered, including the simplest Langmuir, the Bilangmuir and the Tóth isotherm. Based on the statistical evaluation of results according to Fisher's test, IM has shown that the most suitable model to describe the separation of TSO enantiomers on Whelk-O1 CSPs is the Bilangmuir isotherm for all MP compositions but 100% hexane (see later on). In Figure 1, overloaded profiles obtained through IM calculations with a Bilangmuir isotherm (continuous lines) are overlapped to experimental peaks (with points). As it can be seen, in all cases the agreement between experimental and calculated peaks is very consistent.

Table 2 lists the Bilangmuir isotherm parameters as a function of the percentage of ethanol in MP (from 10 to 3%, v/v) for the three columns used in this work.

4.1. 1.8 and 2.5 µm FPPs

The first thing that can be observed by data in Table 2 is that both binding constants and saturation capacity on selective (q_{sel}) and nonselective (q_{nsel}) sites are very similar on the columns packed with FPPs (FFP-2.5 and FFP-1.8). This is, therefore, consistent with the loading of chiral selector measured through elemental analysis (see Table 1). On another viewpoint, it is a confirmation that preparation of Whelk-O1 CSPs, even when based on particles of very reduced dimensions, is a very reproducible and robust process. Finally, it offers a sound thermodynamic explanation for the observation that not only retention (see k_1 values on the third column of Table 3) but also selectivity (fourth column of the same Table) measured at the different MPs under linear conditions are essentially equal on the columns packed with FPPs. Following Fornstedt et al. [41, 42], selectivity measured through retention factors will be denoted by the symbol α_{app}:

$$\alpha_{app} = \frac{k_2}{k_1} \tag{10}$$

where the subscript *app* serves to underline that, when measured this way, enantioselectivity comes from a combination of both selective and nonselective interactions. Therefore, it is an apparent value. On the other hand, the so-called "true" enantioselectivity (α_{true}), based only on enantioselective contributions, can be estimated once isotherm parameters are known (see later on). For the sake of clarity, it is worth clarifying the use of the term "true" applied to the concept of liquid chiral separations on CSPs. As it was pointed out before, chemically modified (chiral) surfaces are intrinsically heterogeneous in terms of their morphology, chemical composition and "solvation" status (which strongly depends on the mobile phase composition). SP and FP porous silica types, in addition, are different and thus also the morphology of the modified silica surface. All of these variables/conditions may have an effect on an experimentally observed enantioselectivity. The word "true", therefore, must not use be considered as an "absolute" concept. It merely describes, under specific conditions, the contribution of the stereoselective and non-stereoselective portfolio of "intermolecular" interactions taking place at the solvated and stereochemically modified silica surface with the chiral analytes.

4.1.1. *The effect of the strong MP modifier amount on binding constant and saturation capacity. Excess isotherms*

By considering how binding constants and saturation capacity change by changing the amount of ethanol (Table 2), some interesting features can be evidenced. Firstly, one may see that selective binding constants for the first eluted enantiomer ($b_{1,sel}$) are essentially independent on the amount of ethanol (they are between 0.010 and 0.013 L/g). On the other hand, increasing ethanol percentage provokes a significant decreasing not only of the enantioselective binding of the more retained enantiomer ($b_{2,sel}$ decreases by almost 60% by moving from 3 to 10% ethanol, v/v in MP), but also of nonselective binding, even if to a smaller extent (b_{nsel} decreases of about 35% for the same change in MP composition). The other interesting observation is about the behavior of saturation capacity with the percentage of ethanol. Surprisingly, indeed saturation capacities of selective sites, q_{sel}, and of nonselective ones, q_{nsel}, exhibit opposite trends. While q_{sel} decreases by almost 30% by decreasing the percentage of ethanol in MP from 10 to 3% v/v (by roughly passing from 42 to 30 g/L), q_{nsel} increases by roughly 10% (from about 98 to 110 g/L). Therefore, the overall effect on retention of selective sites is that, by increasing the amount of ethanol in MP, the Henry's constant of adsorption (see Eq. 7) of the first enantiomer ($a_1 = q_{sel}b_{1,sel}$) slightly increases while that of the second one ($a_2 = q_{sel}b_{2,sel}$) decreases. In addition, nonselective contributions lead to a decrease of retention due to the simultaneous reduction of both binding constant and saturation capacity. The combination of both selective and nonselective contributions leads to the trend observed in Figure 1 (see figure caption for details), where retention decreases with increasing ethanol in MP.

Figure 2 reports the excess isotherm for ethanol/hexane binary mixtures on the three chiral CSPs employed in this work. Details on how excess isotherms were measured are given under SI. Excess isotherms allow to describe the preferential adsorption of ethanol on the stationary phase in function of the bulk MP composition. Basically, the interpretation of these plots reveals that the composition of the stationary phase can be considered constant (and thus independent on the bulk MP composition) only when percentage of ethanol in MP exceeds 10-15% v/v (i.e., when excess isotherms decrease almost linearly with increasing ethanol amount). In this region, our understanding is that ethanol has saturated all polar sites on the surface. It is where a "true" NP chromatographic behavior is effective and retention decreases – following the increase of the strong MP modifier – due to the increasing competition for adsorption on the po-

lar surface by MP modifier molecules [33, 46–49]. On the other hand, in the initial part of isotherms, the composition of stationary phase is not constant but changes with the amount of ethanol in MP. Herein more complex, so-called "mixed-mode" mechanisms can be active which can explain the observed features. Excess isotherms could therefore offer a thermodynamic-based interpretation to the behavior of binding constant and saturation capacity previously observed. Existence of mechanisms affecting retention in opposite ways can also be at the origin of the well known but little understood phenomenon in chiral liquid chromatography, that is the inversion of elution order of enantiomers by changing either MP composition or modifier [50–52].

4.2. Comparison between FPPs and 2.6 µm SPPs

The same general dependence of both saturation capacity and binding constant on the strong MP modifier has been observed also for the chiral SPPs, as shown by data in Table 2.

On the other hand, if one compares fully- and superficially-porous particles at the same MP composition, it can be seen that SPPs are characterized by larger selective and nonselective binding than FPPs. This therefore seems to correlate with the specific loading of chiral selector, which is larger on SPPs than on FPPs (see Table 1).

This could be due to the fact that high selector loading may be responsible, as expected, for an higher contribution of selective sites but, on the other hand, it could also lead to the formation of different structures of chiral selector bonded to the surface that can interact with enantiomers in different manners. This sort of clusters or aggregates between two or more chiral selectors could possibly behave also as nonselective sites. Another hypothesis that can be made is about the existance of secondary interactions between enantiomers and chemical neighborood of the chiral selector that can be different on FPPs or SPPs. However, it is difficult to predict what happens at a molecular level and which kinds of interactions can be involved. More physically-sound explanations can be deduced by performing more speficic measurements (e.g. solid NMR) [53].

This finding is of remarkable interest when considering the employment of these particles in high-efficient ultrafast separations for which they have been originally designed. It is evident indeed that a larger binding constant provokes (on average) longer adsorption-desorption times, which negatively impacts on the *c*-term of the van Deemter equation [1, 2, 28].

The other interesting observation comes from the comparison of saturation capacities. It is evident, indeed, that they are significantly lower (roughly -40%) on superficially- than on fully-porous particles. It is worth

noting that saturation capacity values reported for SPPs are referred only to the porous zone of particles (see details under SI) so that, in principle, one should not expect this large difference. Therefore a possible explanation could be the significantly smaller particle porosity and the following reduced access to intraparticle volume, of SPPs than FPPs (Table 1).
Data reported in Table 2, finally, allows also to calculate the so-called "true" enantioselectivity (see before) defined by [42]:

$$\alpha_{true} = \frac{b_{2,sel}}{b_{1,sel}} \tag{11}$$

α_{true} values are reported in Table 3 next to their corresponding α_{app}s (see Eq. 10). It is interesting to observe that in all cases true enantioselectivity is larger on fully porous particles. This is due to the large binding constant of first eluted enantiomer on selective sites of SPPs, which is on average more than twice as large as that on FPPs.

4.3. Adsorption equilibria with pure hexane

In the last part of this study the behavior of TSO enantiomers with a MP made of pure hexane has been investigated. As it was previously mentioned, in this case the Bilangmuir model did not allow an accurate fitting of overloaded profiles. This means that an heterogeneous model based on the existence of only two different adsorption sites is not satisfactory to account for the heterogeneity of the surface when ethanol is not a MP component. As a matter of fact, the competitive adsorption by ethanol makes the surface "more homogenous" by masking the most polar sites of the surface. Figure 3 show the experimental overloaded band profiles (points) obtained on the three columns with pure hexane MP (see figure captions for more information). As it can be seen, especially for second eluted peaks, tailing is much more pronounced than with binary MPs (see Figure 3). In the same figures, continuous lines represent the overloaded peaks calculated by solving the IM by means of the Tóth isotherm (eq. 8), which assumes a continuous adsorption energy distribution function. Table 4 summarizes the isotherm parameters obtained in this case. Even if, from a theoretical viewpoint, the adsorption model used with pure hexane is very different from that employed with binary MPs, the main information derivable from these parameters is consistent with that obtained with the simpler Bilangmuir isotherm. First of all, indeed, isotherm parameters for the two CSPs made of FPPs are very close each other. In addition, by comparing FPPs and SPPs, it can be observed that, for both enantiomers, binding constants are larger on SPPs, while saturation capacity is

smaller. This thus confirms the intrinsic difference between chiral fully- and superficially-porous Whelk-O1 particles.

5. Conclusions

The investigation of adsorption isotherms of enantiomers on new generation CSPs is a fundamental tool for the deep characterization of the adsorption properties of these phases and possibly for finding correlations between their chemico-physical characteristics (bonding density of chiral selector, porosity, etc.) and thermodynamic quantities that directly affect the enantiorecognition process (such as binding constants on selective and nonselective sites, saturation capacity, adsorption energy distribution function, etc.).
This approach may help to investigate some very important unanswered questions such as whether chiral recognition process is the same on fully- or superficially-porous particles (functionalized with the same chiral selector), how enantiorecognition changes by changing experimental variables (e.g. mobile phase composition), if and how loading of chiral selector affects enantiorecognition, etc.
Combined with studies on the efficiency of these CSPs and mass transfer through them, this information can help not only to understand the complexity of enantioseparations but also to drive further the development of particles, either fully- or superficially-porous, with enhanced kinetic and thermodynamic properties.

6. Acknowledgements

Authors acknowledge dr. Ercolina Bianchini of the University of Ferrara for technical support.

7. Figures and Tables

Figure captions

Fig 1. Experimental (empty circles) and calculated (full lines) overloaded profiles of TSO enantiomers on FPP-1.8 (top), FPP-2.5 (middle) and SPP-2.6 (bottom) columns measured at 90:10 (blue), 92:8 (red), 95:5 (green) and 97:3 (yellow) % (v/v) of hexane/ethanol. Injected concentration: 40 g/L.

Fig 2. Excess adsorption isotherms on the three columns employed in this work (see text for details), expressed as excess volume of ethanol adsorbed on the stationary phase (V_{EtOH}^{exc}) as a function of percentage (v/v) of EtOH (% EtOH) in the mobile phase. Experimental (full circles), fitted curves (full lines).

Fig 3. Experimental (empty circles) and calculated (full line) overloaded profiles of TSO enantiomers on FPP-1.8 (top), FPP-2.5 (middle) and SPP-2.6 (bottom) columns measured at 100% hexane MP. Injected concentration: 40 g/L.

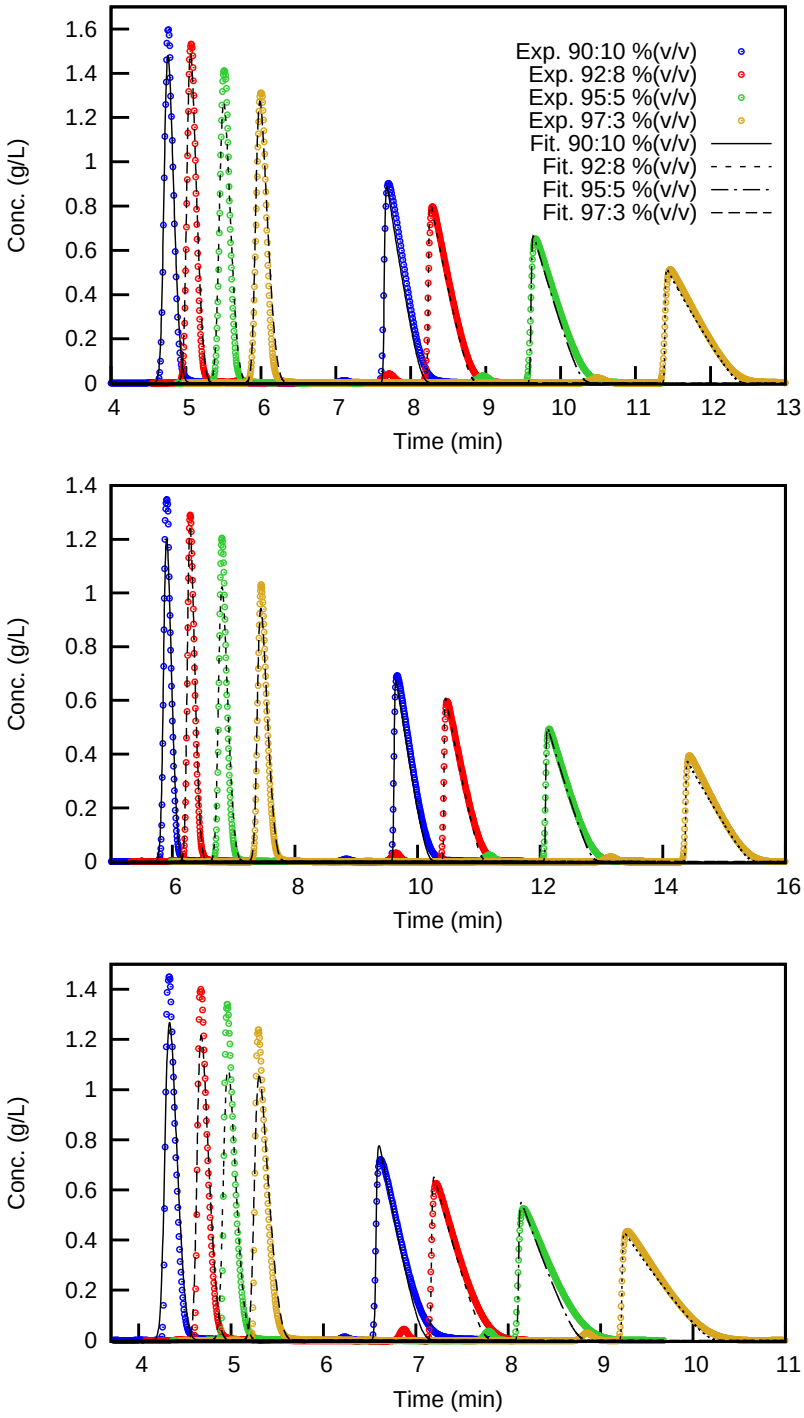
Exp. 90:10 %(v/v)
Exp. 92:8 %(v/v)
Exp. 95:5 %(v/v)
Exp. 97:3 %(v/v)
Fit. 90:10 %(v/v)
Fit. 92:8 %(v/v)
Fit. 95:5 %(v/v)
Fit. 97:3 %(v/v)
Conc. (g/L)
Time (min)

Figure 1:

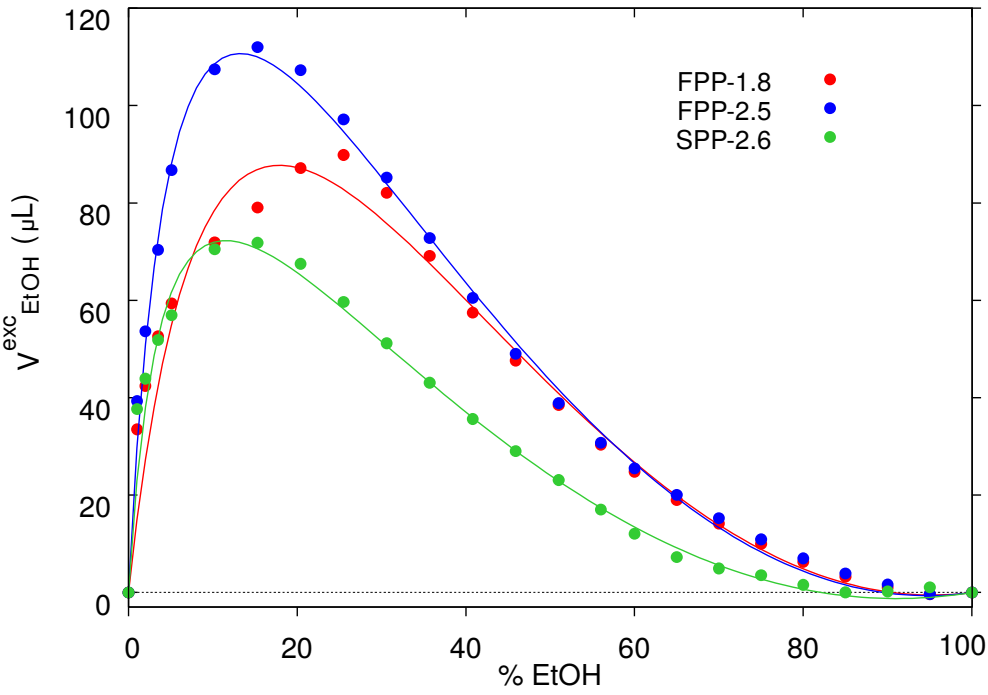
120
100
80
60
40
20
0
0
20
40
60
80
100
% EtOH
V^{exc}_{EtOH} (µL)
FPP-1.8
FPP-2.5
SPP-2.6

Figure 2:

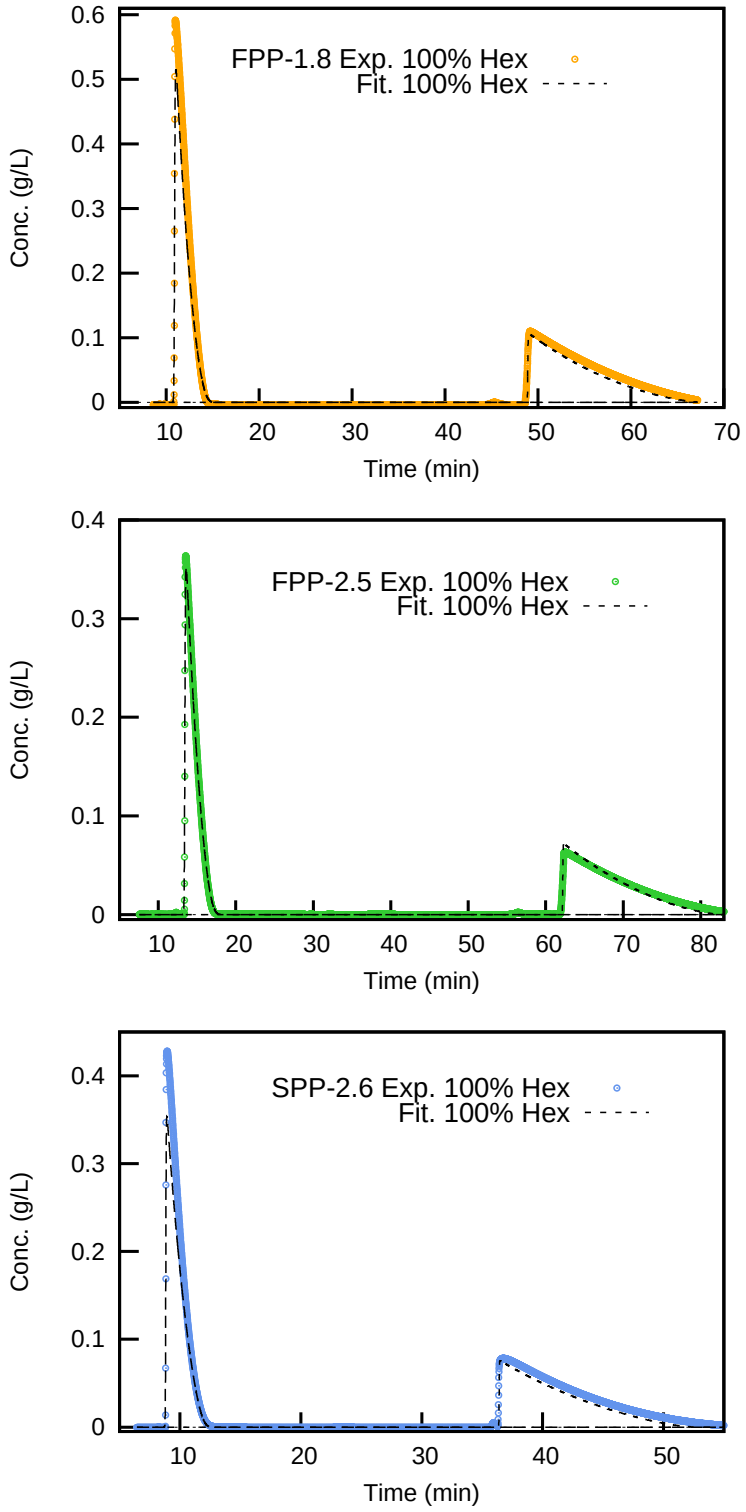
FPP-1.8 Exp. 100% Hex
Fit. 100% Hex
Conc. (g/L)
Time (min)
FPP-2.5 Exp. 100% Hex
Fit. 100% Hex
Conc. (g/L)
Time (min)
SPP-2.6 Exp. 100% Hex
Fit. 100% Hex
Conc. (g/L)
Time (min)

Figure 3:

Table 1: Acronyms of columns employed in this work and their dimensions (length times internal diameter). Chemico-physical characteristics of particles: base silica brand, particle diameter, d_p, specific surface area, A_s, pore size, bonding density (given both as μmol per gram of base silica and μmol per square meter) and particle porosity, ϵ_p.

Column acronym	Dimensions (L×I.D., mm)	Silica brand	d_p (μm)	A_s (m^2/g)	Pore size (Å)	Bonding density (μmol/g)	Bonding density (μmol/m^2)	ϵ_p
FPP-1.8	100×4.6	Kromasil	1.8	323	100	394.6	1.22	0.414
FPP-2.5	150×4.6	Kromasil	2.5	323	100	391.2	1.21	0.438
SPP-2.6	150×4.6	Accucore	2.6	130	80	189.8	1.46	0.251

Table 2: Bilangmuir isotherm parameters calculated through Inverse Method at different percentage of strong MP modifier

MP (% EtOH)	Column	Selective Site			Nonselective Site	
		q_{sel} (g/L)	$b_{1,sel}$ (L/g)	$b_{2,sel}$ (L/g)	q_{nsel} (g/L)	b_{nsel} (L/g)
10	FPP-1.8	42	0.010	0.063	100	0.012
	FPP-2.5	42	0.011	0.071	96	0.013
	SPP-2.6	22	0.022	0.095	50	0.015
8	FPP-1.8	38	0.011	0.071	101	0.012
	FPP-2.5	41	0.013	0.082	102	0.013
	SPP-2.6	22	0.025	0.105	39	0.019
5	FPP-1.8	40	0.011	0.090	104	0.015
	FPP-2.5	36	0.011	0.111	105	0.017
	SPP-2.6	22	0.024	0.128	50	0.020
3	FPP-1.8	33	0.012	0.142	106	0.018
	FPP-2.5	30	0.013	0.170	108	0.020
	SPP-2.6	15	0.025	0.212	49	0.027

Table 3: Retention factor of first eluted enantiomer (k_1) and apparent (α_{app}) and true (α_{true}) selectivity. See text for more details

Eluent (% EtOH)	Column	k_1	α_{app}	α_{true}
10	FPP-1.8	0.6	2.6	6.3
	FPP-2.5	0.7	2.5	6.4
	SPP-2.6	0.5	2.5	4.4
8	FPP-1.8	0.7	2.7	6.5
	FPP-2.5	0.8	2.7	6.3
	SPP-2.6	0.6	2.7	4.2
5	FPP-1.8	0.8	2.9	8.2
	FPP-2.5	0.9	2.8	10.0
	SPP-2.6	0.7	2.8	5.3
3	FPP-1.8	1.0	3.1	11.6
	FPP-2.5	1.0	3.0	13.2
	SPP-2.6	0.8	3.0	8.5

Table 4: Tóth isotherm parameters calculated through Inverse Method with a MP made of pure hexane

Column	q_s (g/L)	b_1 (L/g)	b_2 (L/g)	ν
FPP-1.8	94	0.110	0.589	0.71
FPP-2.5	96	0.128	0.697	0.71
SPP-2.6	30	0.289	1.425	0.81

References

[1] O. H. Ismail, L. Pasti, A. Ciogli, C. Villani, J. Kocergin, S. Anderson, F. Gasparrini, A. Cavazzini, M. Catani, Pirkle-type chiral stationary phase on core-shell and fully porous particles: Are superficially porous particles always the better choice toward ultrafast high-performance enantioseparations?, J. Chromatogr. A 1466 (2016) 96–104.

[2] M. Catani, O. H. Ismail, F. Gasparrini, M. Antonelli, L. Pasti, N. Marchetti, S. Felletti, A. Cavazzini, Recent advancements and future directions of superficially porous chiral stationary phases for ultrafast high-performance enantioseparations, Analyst 142 (2017) 555–566.

[3] M. Catani, S. Felletti, O. H. Ismail, F. Gasparrini, L. Pasti, N. Marchetti, C. D. Luca, V. Costa, A. Cavazzini, New frontiers and cutting edge applications in ultra high performance liquid chromatography through latest generation superficially porous particles with particular emphasis to the field of chiral separations, Anal. Bioanal. Chem, (2018), https://doi.org/110.1007/s00216-017-0842-4.

[4] D. C. Patel, Z. S. Breitbach, M. F. Wahab, C. L. Barhate, D. W. Armstrong, Gone in seconds: praxis, performance and peculiarities of ultrafast chiral liquid chromatography with superficially porous particles, Anal. Chem. 87 (2015) 9137–9148.

[5] C. L. Barhate, Z. S. Breitbach, E. Costa Pinto, E. L. Regalado, C. J. Welch, D. W. Armstrong, Ultrafast separation of fluorinated and desfluorinated pharmaceuticals using highly efficient and selective chiral selectors bonded to superficially porous particles, J. Chromatogr. A 1426 (2015) 241–247.

[6] D. C. Patel, M. F. Wahab, D. W. Armstrong, Z. S. Breitbach, Advances in high-throughput and high-efficiency chiral liquid chromatographic separations, J. Chromatogr. A 1467 (2016) 2–18.

[7] M. D. Dolzan, D. A. Spudeit, Z. S. Breitbach, W. E. Barber, G. A. Micke, D. W. Armstrong, Comparison of superficially porous and fully porous silica supports used for a cyclofructan 6 hydrophilic interaction liquid chromatographic stationary phase, J. Chromatogr. A 1365 (2014) 124–130.

[8] D. A. Spudeit, M. D. Dolzan, Z. S. Breitbach, W. E. Barber, G. A. Micke, D. W. Armstrong, Superficially porous particles vs. fully porous particles for bonded high performance liquid chromatographic chiral stationary phases: Isopropyl cyclofructan 6, J. Chromatogr. A 1363 (2014) 89–95.

[9] M. F. Wahab, R. M. Wimalasinghe, Y. Wang, C. L. Barhate, D. C. Patel, D. W. Armstrong, Salient sub-second separations, Anal. Chem. 88 (2016) 8821–8826.

[10] R. M. Wimalasinghe, C. A. Weatherly, Z. S. Breitbach, D. W. Armstrong, Hydroxypropyl beta cyclodextrin bonded superficially porous particlebased HILIC stationary phases, J. Liq. Chromatogr. Rel. Tech. 39 (2016) 459–464.

[11] K. Lomsadze, G. Jibuti, T. Farkas, B. Chankvetadze, Comparative high-performance liquid chromatography enantioseparations on polysaccharide based stationary phases prepared by coating totally porous and core-shell silica particles, J. Chromatogr. A 1234 (2012) 50–55.

[12] Q. Kharaishvili, G. Jibuti, T. Farkas, B. Chankvetadze, Further proof to the utility of polysaccharide-based chiral selectors in combination with superficially porous silica particles as effective chiral stationary phases for separation of enantiomers in high-performance liquid chromatography, J. Chromatogr. A 1467 (2016) 163–168.

[13] O. H. Ismail, M. Antonelli, A. Ciogli, C. Villani, A. Cavazzini, M. Catani, S. Felletti, D. S. Bell, F. Gasparrini, Future perspectives in high efficient and ultrafast chiral liquidchromatography through zwitterionic teicoplanin-based 2μm superficially porous particles, J. Chromatogr. A 1520 (2017) 91–102.

[14] O. H. Ismail, M. Catani, L. Pasti, A. Cavazzini, A. Ciogli, C. Villani, D. Kotoni, F. Gasparrini, D. S. Bell, Experimental evidence of the kinetic performance achievable with columns packed with the new 1.9 μm fully porous particles Titan c_{18}, J. Chromatogr. A 1454 (2016) 86–92.

[15] M. Catani, O. H. Ismail, A. Cavazzini, A. Ciogli, C. Villani, L. Pasti, D. Cabooter, G. Desmet, F. Gasparrini, D. S. Bell, Rationale behind the optimum efficiency of columns packed with the new 1.9 μm fully porous particles titan C_{18}, J. Chromatogr. A 1454 (2016) 78–85.

[16] C. L. Barhate, D. A. Lopez, A. A. Makarov, X. Bu, W. J. Morris, A. Lekhal, R. Hartman, D. W. Armstrong, E. L. Regalado, Macrocyclic glycopeptide chiral selectors bonded to core-shell particles enables enantiopurity analysis of the entire verubecestat synthetic route, J. Chromatogr. A 1539 (2018) 87–92.

[17] L. Sciascera, O. Ismail, A. Ciogli, D. Kotoni, A. Cavazzini, L. Botta, T. Szczerba, J. Kocergin, C. Villani, F. Gasparrini, Expanding the potential of chiral chromatography for high-throughput screening of large compound libraries by means of sub-2 μm Whelk-O1 stationary phase in supercritical fluid conditions, J. Chromatogr. A (2015) 160–168.

[18] D. Kotoni, A. Ciogli, I. D'Acquarica, J. Kocergin, T. Szczerba, H. Ritchie, C. Villani, F. Gasparrini, Enantioselective ultra-high and high performance liquid chromatography: a comparative study of columns based on the Whelk-O1 selector, J. Chromatogr. A 1269 (2012) 226–241.

[19] O. H. Ismail, A. Ciogli, C. Villani, M. D. Martino, M. Pierini, A. Cavazzini, D. S. Bell, F. Gasparrini, Ultra-fast high-efficiency enantioseparations by means of a teicoplanin-based chiral stationary phase made on sub-2 μm totally porous silica particles of narrow size distribution, J. Chromatogr. A 1427 (2016) 55–68.

[20] L. Bezhitashvili, A. Bardavelidze, T. Ordjonikidze, L. Chankvetadze, M. Chity, T. Farkas, B. Chankvetadze, Effect of pore-size optimization on the performance of polysaccharide-based superficially porous chiral stationary phases for the separation of enantiomers in high-performance liquid chromatography, J. Chromatogr. A 1482 (2017) 32–38.

[21] F. Gritti, G. Guiochon, Mass transfer kinetics, band broadening and column efficiency, J. Chromatogr. A 1221 (2012) 2–40.

[22] A. Felinger, Determination of rate constants for heterogeneous mass transfer kinetics in liquid chromatography, J. Chromatogr. A 1126 (2006) 120–128.

[23] D. C. Patel, Z. S. Breitbach, J. Yu, K. A. Nguyen, D. W. Armstrong, Quinine bonded to superficially porous particles for high-efficiency and ultrafast liquid and supercritical fluid chromatography, Anal. Chim. Acta 963 (2017) 164–174.

[24] A. Cavazzini, F. Gritti, K. Kaczmarski, N. Marchetti, G. Guiochon, Mass-transfer kinetics in a shell packing material for chromatography, Anal. Chem. 79 (2007) 5972–5979.

[25] N. Marchetti, A. Cavazzini, F. Gritti, G. Guiochon, Gradient elution separation and peak capacity of columns packed with porous shell particles, J. Chromatogr. A 1163 (2007) 203–211.

[26] F. Gritti, A. Cavazzini, N. Marchetti, G. Guiochon, Comparison between the efficiencies of columns packed with fully and partially porous C18-bonded silica materials, J. Chromatogr. A 1157 (2007) 289–303.

[27] G. Guiochon, F. Gritti, Shell particles, trials, tribulations and triumphs, J. Chromatogr. A 1218 (2011) 1915–1938.

[28] G. Guiochon, A. Felinger, D. G. Shirazi, A. M. Katti, Fundamentals of Preparative and Nonlinear Chromatography, Academic Press, Elsevier, Second Edition, 2006.

[29] F. Gritti, G. Guiochon, Possible resolution gain in enantioseparations afforded by core-shell particle technology, J. Chromatogr. A 1348 (2014) 87–96.

[30] F. Gritti, G. Guiochon, Mass transfer mechanism in chiral reversed phase liquid chromatography, J. Chromatogr. A 1332 (2014) 35–45.

[31] K. Kaczmarski, A. Cavazzini, P. Szabelski, D. Zhou, X. Liu, G. Guiochon, Application of the general rate model and the generalized Maxwell-Stefan equation to the study of the mass transfer kinetics of a pair of enantiomers, J. Chromatogr. A 962 (2002) 57–67.

[32] A. Felinger, D. M. Zhou, G. Guiochon, Determination of the single component and competitive adsorption isotherms of the 1-indanol enantiomers by the inverse method, J. Chromatogr. A 1005 (2003) 35–49.

[33] M. Catani, R. Guzzinati, N. Marchetti, L. Pasti, A. Cavazzini, Exploring fluorous affinity by liquid chromatography, Anal. Chem. 87 (2015) 6854–6860.

[34] P. Vajda, A. Cavazzini, A. Felinger, Adsorption equilibria of proline in hydrophilic interaction chromatography, J. Chromatogr. A 1217 (2010) 5965–5970.

[35] E. Morgan, K. W. Burton, Optimization using the super-modified simplex method, Chemometr. Intell. Lab. 8 (1990) 97–107.

[36] A. Cavazzini, M. Remelli, F. Dondi, Stochastic theory of two-site adsorption chromatography by the characteristic function method, J. Microcol. Sep. 9 (1997) 295–302.

[37] P. Jandera, V. Bačkovská, A. Felinger, Analysis of the band profiles of the enantiomers of phenylglycine in liquid chromatography on bonded teicoplanin columns using the stochastic theory of chromatography, J. Chromatogr. A 919 (2001) 67–77.

[38] D. Zhou, K. Kaczmarski, A. Cavazzini, X. Liu, G. Guiochon, Modeling of the separation of two enantiomers using a microbore column, J. Chromatogr. A 1020 (2003) 199–217.

[39] A. Cavazzini, F. Dondi, A. Jaulmes, C. Vidal-Madjar, A. Felinger, Monte carlo model of nonlinear chromatography: correspondence between the microscopic stochastic model and the microscopic thomas kinetic model, Anal. Chem. 74 (2002) 6269–6278.

[40] A. Cavazzini, M. Remelli, F. Dondi, A. Felinger, Stochastic theory of multiple-site linear adsorption chromatography, Anal. Chem. 71 (1999) 3453–3462.

[41] T. Fornstedt, P. Sajonz, G. Guiochon, A closer study of chiral retention mechanisms, Chirality 10 (1998) 375–381.

[42] G. Götmar, T. Fornstedt, G. Guiochon, Apparent and true enantioselectivity in enantioseparations, Chirality 12 (2000) 558–564.

[43] G. Götmar, T. Fornstedt, M. Andersson, G. Guiochon, Influence of the solute hydrophobicity on the enantioselective adsorption of beta-blockers on a cellulase protein used as the chiral selector, J. Chromatogr. A 905 (2001) 3–17.

[44] F. Gritti, G. Guiochon, Critical contribution of nonlinear chromatography to the understanding of retention mechanism in reversed-phase liquid chromatography, J. Chromatogr. A 1099 (2005) 1–42.

[45] A. Cavazzini, K. Kaczmarski, P. Szabełski, D. M. Zhou, X. D. Liu, G. Guiochon, Modeling of the separation of the enantiomers of 1-phenyl-1-propanol on cellulose tribenzoate, Anal. Chem. 73 (2001) 5704–5715.

[46] N. Marchetti, L. Caciolli, A. Laganà, F. Gasparrini, L. Pasti, F. Dondi, A. Cavazzini, Fluorous affinity chromatography for enrichment and determination of perfluoroalkyl substances, Anal. Chem. 84 (2012) 7138–7145.

[47] A. Cavazzini, N. Marchetti, R. Guzzinati, L. Pasti, A. Ciogli, F. Gasparrini, A. Laganá, Understanding mixed-mode retention mechanisms in liquid chromatography with hydrophobic stationary phases, Anal. Chem. 86 (2014) 4919–4926.

[48] F. Gritti, Y. V. Kazakevich, G. Guiochon, Effect of the surface coverage of endcapped C_{18}-silica on the excess adsorption isotherms of commonly used organic solvents from water in reversed phase liquid chromatography, J. Chromatogr. A 1169 (2007) 111–124.

[49] S. Bocian, P. Vajda, A. Felinger, B. Buszewski, Solvent excess adsorption on the stationary phases for reversed-phase liquid chromatography with polar functional groups, J. Chromatogr. A 1204 (2007) 35–41.

[50] K. Balmér, P. O. Lagerström, B. A. Persson, G. Schill, Reversed retention order and other stereoselective effects in the separation of amino alcohols on Chiralcel OD, J. Chromatogr. 592 (1992) 331–337.

[51] S. Ma, S. Shen, H. Lee, M. Eriksson, X. Zeng, J. Xu, K. Fandrick, N. Yee, C. Senanayake, N. Grinberg, Mechanistic studies on the chiral recognition of polysaccharide-based chiral stationary phases using liquid chromatography and vibrational circular dichroism: Reversal of elution order of N-substituted alpha-methyl phenylalanine esters, J. Chromatogr. A 1216 (2009) 3784–3793.

[52] L. Chankvetadze, N. Ghibradze, M. Karchkhadze, L. Peng, T. Farkas, B. Chankvetadze, Enantiomer elution order reversal of fluorenylmethoxycarbonyl-isoleucine in high-performance liquid chromatography by changing the mobile phase temperature and composition, J. Chromatogr. A 1218 (2011) 6554–6560.

[53] R. Guzzinati, E. Sarti, M. Catani, V. Costa, A. Pagnoni, A. Martucci, E. Rodeghero, D. Capitani, M. Pietrantonio, A. Cavazzini, L. Pasti, Formation of supramolecular clusters at the interface of Zeolite X following the adsorption of rare-earth cations and their impact on the macroscopic properties of the Zeolite, ChemPhysChem (2018) DOI: 10.1002/cphc.201800333.

Highlights

- Adsorption mechanism was studied on superficially- and fully porous- chiral stationary phases.
- Saturation capacity of chiral core-shell particles is lower than that of fully porous ones.
- Binding constants are larger on superficially porous particles than on fully porous ones.
- Binding constants could be dependent from specific loading of chiral selector.
- Strong mobile phase modifier affects selective and nonselective Henry's constants differently.

On the effect of chiral selector loading and mobile phase composition on adsorption properties of latest generation fully- and superficially-porous Whelk-O1 particles for high-efficient ultrafast enantioseparations

Simona Felletti[a], Chiara De Luca[a], Omar H. Ismail[b], Luisa Pasti[a], Valentina Costa[a], Francesco Gasparrini[b], Alberto Cavazzini[a,*], Martina Catani[a,]**

[a]Department of Chemistry and Pharmaceutical Sciences, University of Ferrara, via L. Borsari 46, 44121 Ferrara, Italy
[b]Department of Drug Chemistry and Technology, "Sapienza" University of Rome, P. le Aldo Moro 5, 00185, Rome, Italy

Abstract

The adsorption isotherms of *trans*-stilbene oxide (TSO) enantiomers have been measured under a variety of normal phase (NP) mobile phases (MPs) on three Whelk-O1 chiral stationary phases (CSPs), prepared respectively on 1.8 μm and 2.5 μm fully porous particles (FPPs) and 2.6 μm superficially porous particles (SPPs). Specific loading of chiral selector (moles per square meter) of the two FPPs was about 20% smaller than that of SPPs (even if they were prepared under exactly the same experimental conditions).
Regardless of particle size or format, adsorption was described by means of a Bilangmuir model with ethanol/hexane MPs. On the other hand, in pure hexane, the Tóth isotherm was employed. Interestingly, it was found that selective and nonselective Henry's constants vary in opposite directions by increasing the percentage of strong MP modifier (between 3 and 10%, v/v). Saturation capacity of SPPs (referred only to the porous zone of the particle) was remarkably smaller than those of FPPs. On the other hand, binding constants on both selective and nonselective sites were sig-

*Corresponding author
**Corresponding author
Email addresses: cvz@unife.it (Alberto Cavazzini), ctnmtn@unife.it (Martina Catani)

nificantly larger on SPPs. Finally, a correlation between the specific loading of chiral selector and the binding constants of enantiomers was suggested by data, which can be important also to understand the kinetic behavior of these particles in chiral ultrafast applications.

Keywords: Chiral Stationary Phases; Whelk-O1 selector; Superficially Porous Particles; Sub-2μm Fully Porous Particles; Adsorption Isotherms.

1. Introduction

The design and development of high efficient particles, either sub-2μm fully porous (FPPs) [1–3] or (second-generation) superficially porous (SPPs) ones [4–12], functionalized with chiral selectors, have represented the most important innovation in the last decade in the field of chiral separations by liquid chromatography. Not only have they allowed for the preparation of packed columns with extraordinary kinetic performance – altogether comparable to that of typical reversed-phase (RP) achiral separations [13–15]– but they also have permitted to decrease the analysis time by up to three orders of magnitude (from tenths of minutes to fractions of seconds) [1–5, 12–14, 16–20].

Many remarkable examples showing the very large potential of new generation particles towards high-efficient ultrafast (sub-seconds) enantioseparations have been published [1–12]. Essentially, in all of these studies the key has been to use very short prototype columns (either 10 or even 5 mm long) operated at the maximum flow rate allowed by the equipment (between 5 and 8 mL/min depending on the brand of the instrument). At very large flow rates, the so-called mass transfer term, or *c*-term, of the van Deemter equation dominates over the other mechanisms of band broadening (longitudinal diffusion and eddy dispersion). Differently from what happens in RP achiral chromatography, in chiral chromatography this term accounts not only for diffusion of molecules through the particles of the packed bed (where flow is absent) but also for the adsorption-desorption kinetics. Adsorption-desorption kinetics is negligible in RP achiral chromatography unless very large molecules (such as proteins or large polypeptides) are considered. It has been indeed demonstrated that for small molecules adsorption-desorption is very fast ([21, 22]). On the opposite, the enantiorecognition process can be slow, even if the extent largely depends on the type of chiral selector employed. For instance, it is generally accepted that brush-type chiral selectors, such as the Whelk-O1 type, are "fast" while other kinds of selectors, including macrocyclic glycopeptides and polysaccharides, are "slow". This information basi-

cally comes from molecular spectroscopic investigation (firstly, by NMR). Therefore, it is not unusual that experimental conditions under which it was obtained can be significantly different from those typical of liquid chromatography. Not just because spectroscopic measurements are (very often) performed in homogeneous systems, where both chiral selectors and anaytes are in solution, but also since solvents employed in these measurements can be very different from typical eluents used in liquid chromatography. Thus, these measurements does not account for the effect of several variables that may affect chiral recognition in heterogenous systems (i.e., when the chiral selector is tethered to the surface), such as the chemical composition of the surface around chiral selector, the surface density of chiral selector, pore size and morphology, their accessibility, the competitive effect for adsorption by so-called strong mobile phase (MP) modifiers, etc.

For the reasons explained above, however, these considerations assume great importance for latest generation sub-2μm fully porous and second-generation superficially porous particles. This is particularly so when one wants to compare superficially- and fully-porous particles (functionalized with the same chiral selector) in terms of kinetic perfomance. The common reasoning [8, 23–27] about the alleged superiority, in terms of efficiency, of the former type of particles over their fully porous counterpart is based on the same considerations employed in achiral RP chromatography, namely that eddy dispersion, longitudinal diffusion and solid-liquid mass transfer are smaller on chiral SPPs than on FPPs. Therefore, these conclusions either completely neglect the role of adsorption-desorption kinetics or they implicitly assume that adsorption-desorption kinetics is identical on both kinds of particles. On the other hand, many authors report that functionalization of SPPs and FPPs systematically leads to different specific loading, or density (μmol/m^2) of chiral selectors on the two types of particles, even if their chemical modification is performed under exactly the same experimental conditions [1, 5, 8, 11, 13].

With the purpose of shedding light on some of these aspects, in this work the adsorption isotherms of *trans*-stilbene oxide (TSO) enantiomers have been measured under normal phase (NP) conditions on three different Whelk-O1 chiral stationary phases (CSPs). Two of them were prepared on FPPs (2.5 and 1.8 μm particle diameter, respectively) and the other one on 2.6 μm SPPs [1, 13]. The investigation of adsorption isotherms is fundamental not only to characterize surface heterogeneity (in terms of adsorption energy distribution) but also to investigate if, e.g., the bonding density has an effect on the binding constants of enantiomers and enantioselectivity of CSPs. In addition, since adsorption-desorption kinetics

is strongly influenced by thermodynamic equilibria [28], this information can also be useful to understand the chromatographic behavior of fully- and superficially-porous particles at high flow rates [1, 2, 29–31].

2. Theory

The equilibrium-dispersive (ED) model has often been used to describe chromatographic separations characterized by efficient mass transfer [28]. In this model, instantaneous equilibrium between mobile (MP) and stationary phase (SP) is assumed. Since both thermodynamics of phase equilibria and mass transfer kinetics change with experimental conditions, the only parameter that is conserved during a chromatographic separation (in absence of chemical reaction) is the mass of the injected sample. Therefore, a differential mass balance equation can be written that, for the ED model, includes an apparent lumped dispersion term (D_a) accounting for all the contributions to band broadening observed in linear chromatography:

$$\frac{\partial C_i}{\partial t} + F\frac{\partial q_i}{\partial t} + u\frac{\partial C_i}{\partial z} = D_{a,i}\frac{\partial^2 C_i}{\partial z^2} \tag{1}$$

where the index i indicates ith component of the system. In this equation, C_i and q_i are the concentrations of analyte in MP and SP, respectively, t represents the temporal coordinate and z the spatial one. Finally, u is the MP linear velocity and F the phase ratio:

$$F = \frac{1-\epsilon_t}{\epsilon_t} \tag{2}$$

being ϵ_t the total porosity of the packed bed given by the ratio between the hold-up, V_0, and the geometric volume, V_{col}, of the column. The apparent dispersion coefficient is calculated through the efficiency of the chromatographic peak under analytical conditions:

$$D_{a,i} = \frac{uL}{2N_i} \tag{3}$$

where N is the number of theoretical plates and L the column length. In the case of enantiomeric separations ($i = 1, 2$), the system will be described by two partial differential equations, which are coupled through a competitive isotherm equation, $q_i = f(C_1, C_2)$ (see later on).

2.1. Inverse Method for determination of isotherms

The direct numerical resolution of the system of mass balance equations requires the knowledge of the isotherm. This can be, for instance, evaluated through (competitive) frontal analysis. Contrary, in the so-called Inverse Method (IM) [32–34], isotherm parameters are derived through a procedure based on the iterative resolution of system of mass balance equations (once an isotherm model has been chosen). Isotherm parameters are calculated by minimizing the differences between experimental and calculated chromatograms. Schematically, IM requires the following steps: i) recording of some experimental overloaded profiles; ii) selection of an isotherm model (the shape of overloaded profiles guides this process [28]) and guess of initial parameters; iii) resolution of system of mass balance equations with the adsorption isotherm just selected (to get a calculated chromatogram); iv) comparison between calculated overloaded profiles and experimental ones; v) tuning of isotherm parameters until calculated and experimental profiles match as much as possible. Numerical optimization of isotherm parameters was made by means of the super-modified simplex method described in [32, 35].

To solve the system of mass balance equations, obviously proper initial and boundary conditions must be defined. In this work, the following initial

$$C_i(z, t = 0) = 0 \quad i = 1, 2 \tag{4}$$

and boundary

$$C_i(z = 0, t) = \begin{cases} C_{i,0} & 0 \leq t \leq t_{inj} \quad i = 1, 2 \\ 0 & t > t_{inj} \end{cases} \tag{5}$$

conditions were taken describing, respectively, that at $t = 0$ the column is equilibrated with pure eluent (Eq. 4) and that the injection profile is a rectangular pulse of concentration $C_{i,0}$ ($i = 1, 2$) during the injection time, t_{inj} (Eq. 5).

2.2. Isotherm models

2.2.1. Langmuir isotherm

The Langmuir model is the most frequently used to describe adsorption in liquid chromatography. Based on the Langmuir model, the adsorption surface is assumed to be paved by only one type of adsorption sites (homogeneous adsorption). In addition, adsorption is monolayer and no lateral interactions between adsorbed molecules are possible. In the case the

Langmuir isotherm is used to model chiral separations, not only it is assumed that nonselective interactions have a negligible contribution to retention of enantiomers but also that energies of all possible enantioselective interactions are close enough that they can be averaged. Accordingly, a single adsorption energy and a single adsorption constant can be defined, which characterize all adsorption sites on the surface. (Obviously, average energies and constants are different for the two enantiomers). The competitive Langmuir model applied to the separation of two enantiomers (denoted hereafter 1 and 2) is written as:

$$q_i = \frac{q_s b_i c_i}{1 + b_1 c_1 + b_2 c_2} \qquad i = 1, 2 \tag{6}$$

where q_s is the saturation capacity (equal for both enantiomers [28]) and b_i is the adsorption equilibrium (binding) constant. The product between q_s and b_i defines the so-called Henry's constant of adsorption, a_i (that is the initial slope of the isotherm). Retention factor (under linear condition), k, and Henry's constant are connected by:

$$k = \frac{t_R - t_0}{t_0} = aF \tag{7}$$

where t_R and t_0 are respectively the retention and hold-up time measured under linear conditions.

2.2.2. Tóth isotherm

This isotherm describes heterogeneous adsorption. In particular, it assumes a continuous and possibly wide adsorption energy distribution. Width depends on the value of the so-called heterogeneity parameter, ν ($0 < \nu < 1$). The smaller ν the wider the adsorption energy distribution function. For binary competitive systems, the Tóth isotherm is:

$$q_i = \frac{q_s b_i c_i}{[1 + (b_1 c_1 + b_2 c_2)^\nu]^{1/\nu}} \qquad i = 1, 2 \tag{8}$$

2.2.3. Bilangmuir isotherm

The Bilangmuir model, finally, accounts for a bimodal adsorption energy distribution due to the presence of two different adsorption sites that, in case of chiral separations, are considered selective (responsible for diastereomeric or enantioselective interactions) and nonselective (where both enantiomers behave identically) [36]. This model has been often successfully applied to describe adsorption processes of enantiomers on CSPs

[32, 37, 38]. The competitive 2-component adsorption isotherm is:

$$q_i = \frac{q_{sel} b_{i,sel} c_i}{1 + b_{1,sel} c_1 + b_{2,sel} c_2} + \frac{q_{nsel} b_{nsel} c_i}{1 + b_{nsel}(c_1 + c_2)} \qquad i = 1, 2 \tag{9}$$

where subscripts *sel* and *nsel* refer to selective and nonselective sites, respectively [28, 32, 39, 40].

3. Materials and methods

3.1. Columns and materials

All solvents and reagents were purchased from Sigma Aldrich (St. Louis, MI, USA). Kromasil fully porous silica particles (2.5 and 1.8 μm particle size, 100 Å pore size, 323 m^2/g specific surface area) were from Akzo-Nobel (Bohus, Sweden). Accucore second-generation superficially porous silica particles (2.6 μm, 80 Å pore size, 130 m^2/g specific surface area, radius of core over particle radius, $\rho = 0.63$) were from Thermo Fisher Scientific (Waltham, MA, USA). Whelk-O1 selector was generously donated by Regis Technologies Inc. (Morton Grove, IL, USA). Synthesis and preparation of Whelk-O1 CSPs are reported in Ref. [1]. 100 and 150 mm$\times$4.6 mm empty stainless steel columns were from IsoBar Systems by Idex (Erlangen, Germany).

3.2. Equipment

All measurements were performed on an Agilent 1100 Series Capillary LC system equipped with a binary solvent pump, a column thermostat and a photodiode array detector. An external manual injector (Rheodyne 8125, equipped with either 5 or 50 μL fixed-loops) was used for sample injections. Detector calibration was performed by sequentially injecting 50 μL TSO racemic solutions (concentration from 0.05 g/l to 5 g/L) without the column. This volume was large enouth to observe concentration plateau. Wavelength: 280 nm.

3.3. Experimental conditions

Adsorption isotherms were measured at five different hexane/ethanol MP compositions: 90/10, 92/8, 95/5, 97/3 and 100/0, % v/v. Temperature was 35°C. TSO racemic mixture injected concentrations were: 3, 10, 20, 40, 50 g/L. Injection volume was 5 μL.

4. Results and discussion

Table 1 reports some of the physico-chemical characteristics of particles and columns employed in this work [1, 2, 30]. Fully porous particles were used to prepare the columns named FPP-1.8 and FPP-2.5; the column called SPP-2.6 was packed with core-shell particles (see Table 1). Information on particle diameter, specific surface area and pore size comes from manufacturers. Bonding density was determined through elemental analysis (more information under SI). As expected, bonding densities per gram of base silica are larger on FPPs (for which essentially the same value was obtained regardless of particle size) than on SPPs. On the other hand, specific bonding density (μmol/m^2) is significantly larger (by almost 20%) on SPPs than that of FPPs. This last finding has been observed also with other chiral selectors [13] and by other authors [5, 8]. However, in other cases [7] the opposite was reported so that no generalization can be made. It is worth noting that functionalization of both SPPs and FPPs was performed under identical experimental conditions (and repeated several times). Nevertheless, specific bonding density was different. Among the hypotheses that can be formulated to explain why this happens, the different reactivity of surface silanol groups on the two kinds of particles or the different accessibility of intraparticle space (during particle functionalization) are the most likely. Particle porosity, ϵ_p, was measured as reported under SI. ϵ_p, describing the fraction of empty pores per particle, is consistent with values of specific bonding density.

To investigate whether the different specific bonding density of chiral selector entails changes on the CSPs, the adsorption isotherms of the enantiomers of a probe compound, TSO, were measured under NP conditions. Measuring the isotherms is the only approach to characterize the surface in terms of adsorption sites and their abundance. This information, on the other hand, cannot be gathered through measurements performed under linear conditions (i.e., by means of retention factors) [28, 32, 41–45].

Isotherms were measured through IM. Different competitive adsorption models were considered, including the simplest Langmuir, the Bilangmuir and the Tóth isotherm. Based on the statistical evaluation of results according to Fisher's test, IM has shown that the most suitable model to describe the separation of TSO enantiomers on Whelk-O1 CSPs is the Bilangmuir isotherm for all MP compositions but 100% hexane (see later on). In Figure 1, overloaded profiles obtained through IM calculations with a Bilangmuir isotherm (continuous lines) are overlapped to experimental peaks (with points). As it can be seen, in all cases the agreement between experimental and calculated peaks is very consistent.

Table 2 lists the Bilangmuir isotherm parameters as a function of the percentage of ethanol in MP (from 10 to 3%, v/v) for the three columns used in this work.

4.1. 1.8 and 2.5 µm FPPs

The first thing that can be observed by data in Table 2 is that both binding constants and saturation capacity on selective (q_{sel}) and nonselective (q_{nsel}) sites are very similar on the columns packed with FPPs (FFP-2.5 and FFP-1.8). This is, therefore, consistent with the loading of chiral selector measured through elemental analysis (see Table 1). On another viewpoint, it is a confirmation that preparation of Whelk-O1 CSPs, even when based on particles of very reduced dimensions, is a very reproducible and robust process. Finally, it offers a sound thermodynamic explanation for the observation that not only retention (see k_1 values on the third column of Table 3) but also selectivity (fourth column of the same Table) measured at the different MPs under linear conditions are essentially equal on the columns packed with FPPs. Following Fornstedt et al. [41, 42], selectivity measured through retention factors will be denoted by the symbol α_{app}:

$$\alpha_{app} = \frac{k_2}{k_1} \tag{10}$$

where the subscript *app* serves to underline that, when measured this way, enantioselectivity comes from a combination of both selective and nonselective interactions. Therefore, it is an apparent value. On the other hand, the so-called "true" enantioselectivity (α_{true}), based only on enantioselective contributions, can be estimated once isotherm parameters are known (see later on). For the sake of clarity, it is worth clarifying the use of the term "true" applied to the concept of liquid chiral separations on CSPs. As it was pointed out before, chemically modified (chiral) surfaces are intrinsically heterogeneous in terms of their morphology, chemical composition and "solvation" status (which strongly depends on the mobile phase composition). SP and FP porous silica types, in addition, are different and thus also the morphology of the modified silica surface. All of these variables/conditions may have an effect on an experimentally observed enantioselectivity. The word "true", therefore, must not use be considered as an "absolute" concept. It merely describes, under specific conditions, the contribution of the stereoselective and non-stereoselective portfolio of "intermolecular" interactions taking place at the solvated and stereochemically modified silica surface with the chiral analytes.

4.1.1. *The effect of the strong MP modifier amount on binding constant and saturation capacity. Excess isotherms*

By considering how binding constants and saturation capacity change by changing the amount of ethanol (Table 2), some interesting features can be evidenced. Firstly, one may see that selective binding constants for the first eluted enantiomer ($b_{1,sel}$) are essentially independent on the amount of ethanol (they are between 0.010 and 0.013 L/g). On the other hand, increasing ethanol percentage provokes a significant decreasing not only of the enantioselective binding of the more retained enantiomer ($b_{2,sel}$ decreases by almost 60% by moving from 3 to 10% ethanol, v/v in MP), but also of nonselective binding, even if to a smaller extent (b_{nsel} decreases of about 35% for the same change in MP composition). The other interesting observation is about the behavior of saturation capacity with the percentage of ethanol. Surprisingly, indeed saturation capacities of selective sites, q_{sel}, and of nonselective ones, q_{nsel}, exhibit opposite trends. While q_{sel} decreases by almost 30% by decreasing the percentage of ethanol in MP from 10 to 3% v/v (by roughly passing from 42 to 30 g/L), q_{nsel} increases by roughly 10% (from about 98 to 110 g/L). Therefore, the overall effect on retention of selective sites is that, by increasing the amount of ethanol in MP, the Henry's constant of adsorption (see Eq. 7) of the first enantiomer ($a_1 = q_{sel}b_{1,sel}$) slightly increases while that of the second one ($a_2 = q_{sel}b_{2,sel}$) decreases. In addition, nonselective contributions lead to a decrease of retention due to the simultaneous reduction of both binding constant and saturation capacity. The combination of both selective and nonselective contributions leads to the trend observed in Figure 1 (see figure caption for details), where retention decreases with increasing ethanol in MP.

Figure 2 reports the excess isotherm for ethanol/hexane binary mixtures on the three chiral CSPs employed in this work. Details on how excess isotherms were measured are given under SI. Excess isotherms allow to describe the preferential adsorption of ethanol on the stationary phase in function of the bulk MP composition. Basically, the interpretation of these plots reveals that the composition of the stationary phase can be considered constant (and thus independent on the bulk MP composition) only when percentage of ethanol in MP exceeds 10-15% v/v (i.e., when excess isotherms decrease almost linearly with increasing ethanol amount). In this region, our understanding is that ethanol has saturated all polar sites on the surface. It is where a "true" NP chromatographic behavior is effective and retention decreases – following the increase of the strong MP modifier – due to the increasing competition for adsorption on the po-

lar surface by MP modifier molecules [33, 46–49]. On the other hand, in the initial part of isotherms, the composition of stationary phase is not constant but changes with the amount of ethanol in MP. Herein more complex, so-called "mixed-mode" mechanisms can be active which can explain the observed features. Excess isotherms could therefore offer a thermodynamic-based interpretation to the behavior of binding constant and saturation capacity previously observed. Existence of mechanisms affecting retention in opposite ways can also be at the origin of the well known but little understood phenomenon in chiral liquid chromatography, that is the inversion of elution order of enantiomers by changing either MP composition or modifier [50–52].

4.2. Comparison between FPPs and 2.6 µm SPPs

The same general dependence of both saturation capacity and binding constant on the strong MP modifier has been observed also for the chiral SPPs, as shown by data in Table 2.

On the other hand, if one compares fully- and superficially-porous particles at the same MP composition, it can be seen that SPPs are characterized by larger selective and nonselective binding than FPPs. This therefore seems to correlate with the specific loading of chiral selector, which is larger on SPPs than on FPPs (see Table 1).

This could be due to the fact that high selector loading may be responsible, as expected, for an higher contribution of selective sites but, on the other hand, it could also lead to the formation of different structures of chiral selector bonded to the surface that can interact with enantiomers in different manners. This sort of clusters or aggregates between two or more chiral selectors could possibly behave also as nonselective sites. Another hypothesis that can be made is about the existance of secondary interactions between enantiomers and chemical neighborood of the chiral selector that can be different on FPPs or SPPs. However, it is difficult to predict what happens at a molecular level and which kinds of interactions can be involved. More physically-sound explanations can be deduced by performing more speficic measurements (e.g. solid NMR) [53].

This finding is of remarkable interest when considering the employment of these particles in high-efficient ultrafast separations for which they have been originally designed. It is evident indeed that a larger binding constant provokes (on average) longer adsorption-desorption times, which negatively impacts on the *c*-term of the van Deemter equation [1, 2, 28].

The other interesting observation comes from the comparison of saturation capacities. It is evident, indeed, that they are significantly lower (roughly -40%) on superficially- than on fully-porous particles. It is worth

noting that saturation capacity values reported for SPPs are referred only to the porous zone of particles (see details under SI) so that, in principle, one should not expect this large difference. Therefore a possible explanation could be the significantly smaller particle porosity and the following reduced access to intraparticle volume, of SPPs than FPPs (Table 1).
Data reported in Table 2, finally, allows also to calculate the so-called "true" enantioselectivity (see before) defined by [42]:

$$\alpha_{true} = \frac{b_{2,sel}}{b_{1,sel}} \tag{11}$$

α_{true} values are reported in Table 3 next to their corresponding α_{app}s (see Eq. 10). It is interesting to observe that in all cases true enantioselectivity is larger on fully porous particles. This is due to the large binding constant of first eluted enantiomer on selective sites of SPPs, which is on average more than twice as large as that on FPPs.

4.3. Adsorption equilibria with pure hexane

In the last part of this study the behavior of TSO enantiomers with a MP made of pure hexane has been investigated. As it was previously mentioned, in this case the Bilangmuir model did not allow an accurate fitting of overloaded profiles. This means that an heterogeneous model based on the existence of only two different adsorption sites is not satisfactory to account for the heterogeneity of the surface when ethanol is not a MP component. As a matter of fact, the competitive adsorption by ethanol makes the surface "more homogenous" by masking the most polar sites of the surface. Figure 3 show the experimental overloaded band profiles (points) obtained on the three columns with pure hexane MP (see figure captions for more information). As it can be seen, especially for second eluted peaks, tailing is much more pronounced than with binary MPs (see Figure 3). In the same figures, continuous lines represent the overloaded peaks calculated by solving the IM by means of the Tóth isotherm (eq. 8), which assumes a continuous adsorption energy distribution function. Table 4 summarizes the isotherm parameters obtained in this case. Even if, from a theoretical viewpoint, the adsorption model used with pure hexane is very different from that employed with binary MPs, the main information derivable from these parameters is consistent with that obtained with the simpler Bilangmuir isotherm. First of all, indeed, isotherm parameters for the two CSPs made of FPPs are very close each other. In addition, by comparing FPPs and SPPs, it can be observed that, for both enantiomers, binding constants are larger on SPPs, while saturation capacity is

smaller. This thus confirms the intrinsic difference between chiral fully- and superficially-porous Whelk-O1 particles.

5. Conclusions

The investigation of adsorption isotherms of enantiomers on new generation CSPs is a fundamental tool for the deep characterization of the adsorption properties of these phases and possibly for finding correlations between their chemico-physical characteristics (bonding density of chiral selector, porosity, etc.) and thermodynamic quantities that directly affect the enantiorecognition process (such as binding constants on selective and nonselective sites, saturation capacity, adsorption energy distribution function, etc.).
This approach may help to investigate some very important unanswered questions such as whether chiral recognition process is the same on fully- or superficially-porous particles (functionalized with the same chiral selector), how enantiorecognition changes by changing experimental variables (e.g. mobile phase composition), if and how loading of chiral selector affects enantiorecognition, etc.
Combined with studies on the efficiency of these CSPs and mass transfer through them, this information can help not only to understand the complexity of enantioseparations but also to drive further the development of particles, either fully- or superficially-porous, with enhanced kinetic and thermodynamic properties.

6. Acknowledgements

Authors acknowledge dr. Ercolina Bianchini of the University of Ferrara for technical support.

7. Figures and Tables

Figure captions

Fig 1. Experimental (empty circles) and calculated (full lines) overloaded profiles of TSO enantiomers on FPP-1.8 (top), FPP-2.5 (middle) and SPP-2.6 (bottom) columns measured at 90:10 (blue), 92:8 (red), 95:5 (green) and 97:3 (yellow) % (v/v) of hexane/ethanol. Injected concentration: 40 g/L.

Fig 2. Excess adsorption isotherms on the three columns employed in this work (see text for details), expressed as excess volume of ethanol adsorbed on the stationary phase (V_{EtOH}^{exc}) as a function of percentage (v/v) of EtOH (% EtOH) in the mobile phase. Experimental (full circles), fitted curves (full lines).

Fig 3. Experimental (empty circles) and calculated (full line) overloaded profiles of TSO enantiomers on FPP-1.8 (top), FPP-2.5 (middle) and SPP-2.6 (bottom) columns measured at 100% hexane MP. Injected concentration: 40 g/L.

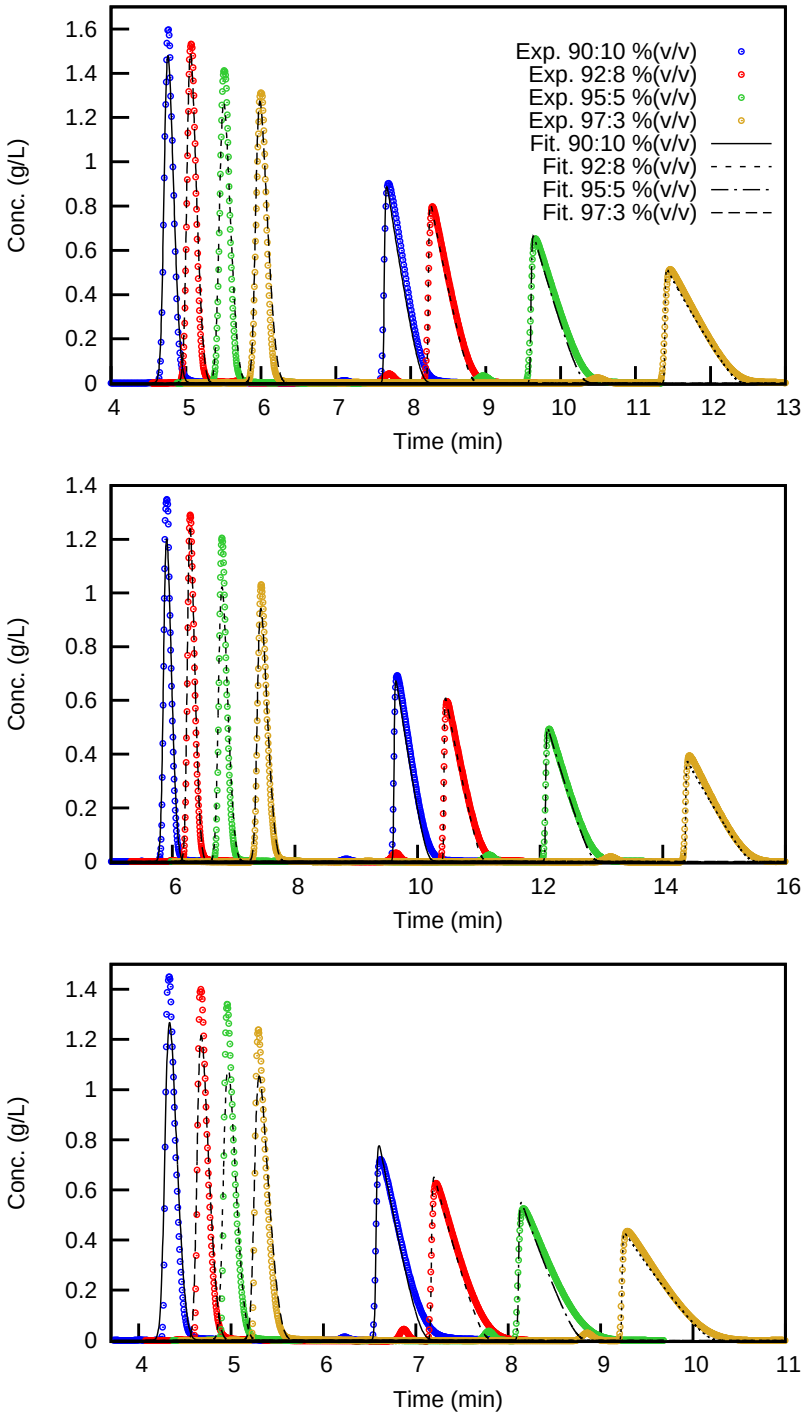
Exp. 90:10 %(v/v)
Exp. 92:8 %(v/v)
Exp. 95:5 %(v/v)
Exp. 97:3 %(v/v)
Fit. 90:10 %(v/v)
Fit. 92:8 %(v/v)
Fit. 95:5 %(v/v)
Fit. 97:3 %(v/v)
Conc. (g/L)
Time (min)

Figure 1:

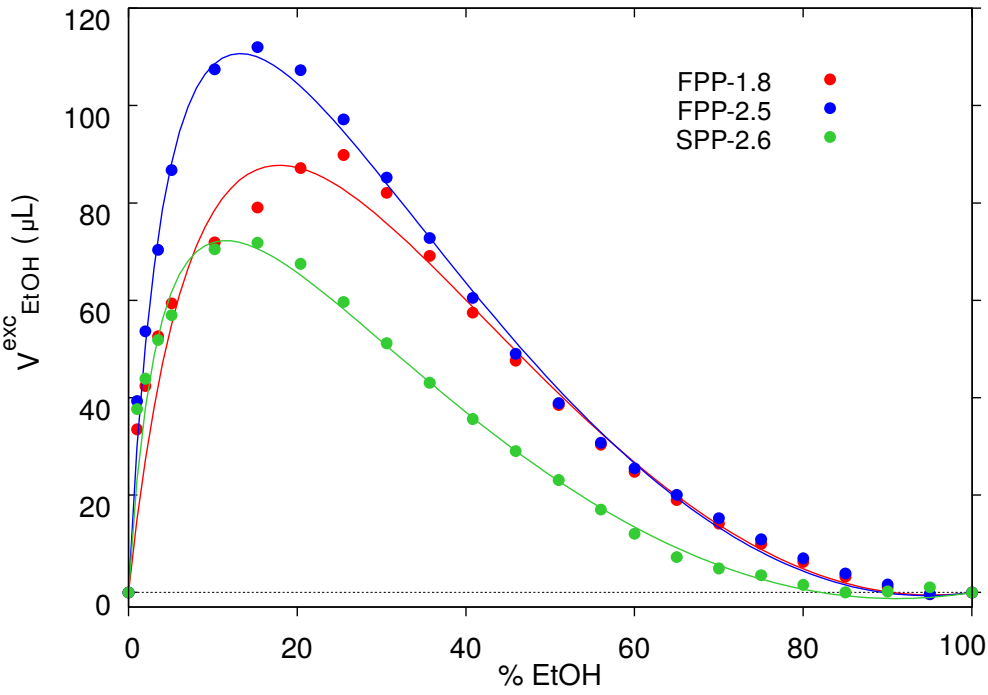
120
100
80
60
40
20
0
0
20
40
60
80
100
% EtOH
V^{exc}_{EtOH} (µL)
FPP-1.8
FPP-2.5
SPP-2.6

Figure 2:

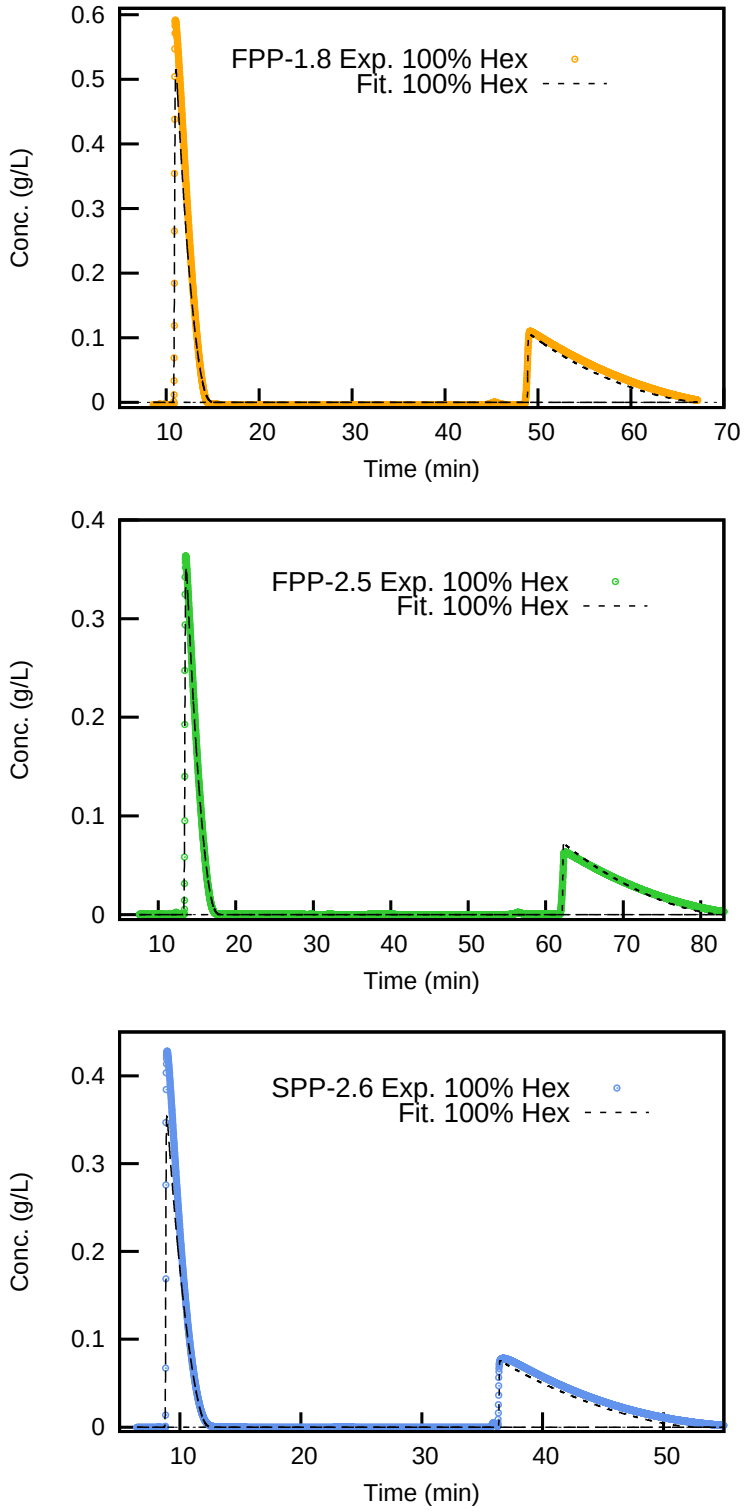
FPP-1.8 Exp. 100% Hex
Fit. 100% Hex
Conc. (g/L)
Time (min)
FPP-2.5 Exp. 100% Hex
Fit. 100% Hex
Conc. (g/L)
Time (min)
SPP-2.6 Exp. 100% Hex
Fit. 100% Hex
Conc. (g/L)
Time (min)

Figure 3:

Table 1: Acronyms of columns employed in this work and their dimensions (length times internal diameter). Chemico-physical characteristics of particles: base silica brand, particle diameter, d_p, specific surface area, A_s, pore size, bonding density (given both as μmol per gram of base silica and μmol per square meter) and particle porosity, ϵ_p.

Column acronym	Dimensions (L×I.D., mm)	Silica brand	d_p (μm)	A_s (m^2/g)	Pore size (Å)	Bonding density (μmol/g)	Bonding density (μmol/m^2)	ϵ_p
FPP-1.8	100×4.6	Kromasil	1.8	323	100	394.6	1.22	0.414
FPP-2.5	150×4.6	Kromasil	2.5	323	100	391.2	1.21	0.438
SPP-2.6	150×4.6	Accucore	2.6	130	80	189.8	1.46	0.251

Table 2: Bilangmuir isotherm parameters calculated through Inverse Method at different percentage of strong MP modifier

MP (% EtOH)	Column	Selective Site			Nonselective Site	
		q_{sel} (g/L)	$b_{1,sel}$ (L/g)	$b_{2,sel}$ (L/g)	q_{nsel} (g/L)	b_{nsel} (L/g)
10	FPP-1.8	42	0.010	0.063	100	0.012
	FPP-2.5	42	0.011	0.071	96	0.013
	SPP-2.6	22	0.022	0.095	50	0.015
8	FPP-1.8	38	0.011	0.071	101	0.012
	FPP-2.5	41	0.013	0.082	102	0.013
	SPP-2.6	22	0.025	0.105	39	0.019
5	FPP-1.8	40	0.011	0.090	104	0.015
	FPP-2.5	36	0.011	0.111	105	0.017
	SPP-2.6	22	0.024	0.128	50	0.020
3	FPP-1.8	33	0.012	0.142	106	0.018
	FPP-2.5	30	0.013	0.170	108	0.020
	SPP-2.6	15	0.025	0.212	49	0.027

Table 3: Retention factor of first eluted enantiomer (k_1) and apparent (α_{app}) and true (α_{true}) selectivity. See text for more details

Eluent (% EtOH)	Column	k_1	α_{app}	α_{true}
10	FPP-1.8	0.6	2.6	6.3
	FPP-2.5	0.7	2.5	6.4
	SPP-2.6	0.5	2.5	4.4
8	FPP-1.8	0.7	2.7	6.5
	FPP-2.5	0.8	2.7	6.3
	SPP-2.6	0.6	2.7	4.2
5	FPP-1.8	0.8	2.9	8.2
	FPP-2.5	0.9	2.8	10.0
	SPP-2.6	0.7	2.8	5.3
3	FPP-1.8	1.0	3.1	11.6
	FPP-2.5	1.0	3.0	13.2
	SPP-2.6	0.8	3.0	8.5

Table 4: Tóth isotherm parameters calculated through Inverse Method with a MP made of pure hexane

Column	q_s (g/L)	b_1 (L/g)	b_2 (L/g)	ν
FPP-1.8	94	0.110	0.589	0.71
FPP-2.5	96	0.128	0.697	0.71
SPP-2.6	30	0.289	1.425	0.81

References

[1] O. H. Ismail, L. Pasti, A. Ciogli, C. Villani, J. Kocergin, S. Anderson, F. Gasparrini, A. Cavazzini, M. Catani, Pirkle-type chiral stationary phase on core-shell and fully porous particles: Are superficially porous particles always the better choice toward ultrafast high-performance enantioseparations?, J. Chromatogr. A 1466 (2016) 96–104.

[2] M. Catani, O. H. Ismail, F. Gasparrini, M. Antonelli, L. Pasti, N. Marchetti, S. Felletti, A. Cavazzini, Recent advancements and future directions of superficially porous chiral stationary phases for ultrafast high-performance enantioseparations, Analyst 142 (2017) 555–566.

[3] M. Catani, S. Felletti, O. H. Ismail, F. Gasparrini, L. Pasti, N. Marchetti, C. D. Luca, V. Costa, A. Cavazzini, New frontiers and cutting edge applications in ultra high performance liquid chromatography through latest generation superficially porous particles with particular emphasis to the field of chiral separations, Anal. Bioanal. Chem, (2018), https://doi.org/110.1007/s00216-017-0842-4.

[4] D. C. Patel, Z. S. Breitbach, M. F. Wahab, C. L. Barhate, D. W. Armstrong, Gone in seconds: praxis, performance and peculiarities of ultrafast chiral liquid chromatography with superficially porous particles, Anal. Chem. 87 (2015) 9137–9148.

[5] C. L. Barhate, Z. S. Breitbach, E. Costa Pinto, E. L. Regalado, C. J. Welch, D. W. Armstrong, Ultrafast separation of fluorinated and desfluorinated pharmaceuticals using highly efficient and selective chiral selectors bonded to superficially porous particles, J. Chromatogr. A 1426 (2015) 241–247.

[6] D. C. Patel, M. F. Wahab, D. W. Armstrong, Z. S. Breitbach, Advances in high-throughput and high-efficiency chiral liquid chromatographic separations, J. Chromatogr. A 1467 (2016) 2–18.

[7] M. D. Dolzan, D. A. Spudeit, Z. S. Breitbach, W. E. Barber, G. A. Micke, D. W. Armstrong, Comparison of superficially porous and fully porous silica supports used for a cyclofructan 6 hydrophilic interaction liquid chromatographic stationary phase, J. Chromatogr. A 1365 (2014) 124–130.

[8] D. A. Spudeit, M. D. Dolzan, Z. S. Breitbach, W. E. Barber, G. A. Micke, D. W. Armstrong, Superficially porous particles vs. fully porous particles for bonded high performance liquid chromatographic chiral stationary phases: Isopropyl cyclofructan 6, J. Chromatogr. A 1363 (2014) 89–95.

[9] M. F. Wahab, R. M. Wimalasinghe, Y. Wang, C. L. Barhate, D. C. Patel, D. W. Armstrong, Salient sub-second separations, Anal. Chem. 88 (2016) 8821–8826.

[10] R. M. Wimalasinghe, C. A. Weatherly, Z. S. Breitbach, D. W. Armstrong, Hydroxypropyl beta cyclodextrin bonded superficially porous particlebased HILIC stationary phases, J. Liq. Chromatogr. Rel. Tech. 39 (2016) 459–464.

[11] K. Lomsadze, G. Jibuti, T. Farkas, B. Chankvetadze, Comparative high-performance liquid chromatography enantioseparations on polysaccharide based stationary phases prepared by coating totally porous and core-shell silica particles, J. Chromatogr. A 1234 (2012) 50–55.

[12] Q. Kharaishvili, G. Jibuti, T. Farkas, B. Chankvetadze, Further proof to the utility of polysaccharide-based chiral selectors in combination with superficially porous silica particles as effective chiral stationary phases for separation of enantiomers in high-performance liquid chromatography, J. Chromatogr. A 1467 (2016) 163–168.

[13] O. H. Ismail, M. Antonelli, A. Ciogli, C. Villani, A. Cavazzini, M. Catani, S. Felletti, D. S. Bell, F. Gasparrini, Future perspectives in high efficient and ultrafast chiral liquidchromatography through zwitterionic teicoplanin-based 2μm superficially porous particles, J. Chromatogr. A 1520 (2017) 91–102.

[14] O. H. Ismail, M. Catani, L. Pasti, A. Cavazzini, A. Ciogli, C. Villani, D. Kotoni, F. Gasparrini, D. S. Bell, Experimental evidence of the kinetic performance achievable with columns packed with the new 1.9 μm fully porous particles Titan c_{18}, J. Chromatogr. A 1454 (2016) 86–92.

[15] M. Catani, O. H. Ismail, A. Cavazzini, A. Ciogli, C. Villani, L. Pasti, D. Cabooter, G. Desmet, F. Gasparrini, D. S. Bell, Rationale behind the optimum efficiency of columns packed with the new 1.9 μm fully porous particles titan C_{18}, J. Chromatogr. A 1454 (2016) 78–85.

[16] C. L. Barhate, D. A. Lopez, A. A. Makarov, X. Bu, W. J. Morris, A. Lekhal, R. Hartman, D. W. Armstrong, E. L. Regalado, Macrocyclic glycopeptide chiral selectors bonded to core-shell particles enables enantiopurity analysis of the entire verubecestat synthetic route, J. Chromatogr. A 1539 (2018) 87–92.

[17] L. Sciascera, O. Ismail, A. Ciogli, D. Kotoni, A. Cavazzini, L. Botta, T. Szczerba, J. Kocergin, C. Villani, F. Gasparrini, Expanding the potential of chiral chromatography for high-throughput screening of large compound libraries by means of sub-2 μm Whelk-O1 stationary phase in supercritical fluid conditions, J. Chromatogr. A (2015) 160–168.

[18] D. Kotoni, A. Ciogli, I. D'Acquarica, J. Kocergin, T. Szczerba, H. Ritchie, C. Villani, F. Gasparrini, Enantioselective ultra-high and high performance liquid chromatography: a comparative study of columns based on the Whelk-O1 selector, J. Chromatogr. A 1269 (2012) 226–241.

[19] O. H. Ismail, A. Ciogli, C. Villani, M. D. Martino, M. Pierini, A. Cavazzini, D. S. Bell, F. Gasparrini, Ultra-fast high-efficiency enantioseparations by means of a teicoplanin-based chiral stationary phase made on sub-2 μm totally porous silica particles of narrow size distribution, J. Chromatogr. A 1427 (2016) 55–68.

[20] L. Bezhitashvili, A. Bardavelidze, T. Ordjonikidze, L. Chankvetadze, M. Chity, T. Farkas, B. Chankvetadze, Effect of pore-size optimization on the performance of polysaccharide-based superficially porous chiral stationary phases for the separation of enantiomers in high-performance liquid chromatography, J. Chromatogr. A 1482 (2017) 32–38.

[21] F. Gritti, G. Guiochon, Mass transfer kinetics, band broadening and column efficiency, J. Chromatogr. A 1221 (2012) 2–40.

[22] A. Felinger, Determination of rate constants for heterogeneous mass transfer kinetics in liquid chromatography, J. Chromatogr. A 1126 (2006) 120–128.

[23] D. C. Patel, Z. S. Breitbach, J. Yu, K. A. Nguyen, D. W. Armstrong, Quinine bonded to superficially porous particles for high-efficiency and ultrafast liquid and supercritical fluid chromatography, Anal. Chim. Acta 963 (2017) 164–174.

[24] A. Cavazzini, F. Gritti, K. Kaczmarski, N. Marchetti, G. Guiochon, Mass-transfer kinetics in a shell packing material for chromatography, Anal. Chem. 79 (2007) 5972–5979.

[25] N. Marchetti, A. Cavazzini, F. Gritti, G. Guiochon, Gradient elution separation and peak capacity of columns packed with porous shell particles, J. Chromatogr. A 1163 (2007) 203–211.

[26] F. Gritti, A. Cavazzini, N. Marchetti, G. Guiochon, Comparison between the efficiencies of columns packed with fully and partially porous C18-bonded silica materials, J. Chromatogr. A 1157 (2007) 289–303.

[27] G. Guiochon, F. Gritti, Shell particles, trials, tribulations and triumphs, J. Chromatogr. A 1218 (2011) 1915–1938.

[28] G. Guiochon, A. Felinger, D. G. Shirazi, A. M. Katti, Fundamentals of Preparative and Nonlinear Chromatography, Academic Press, Elsevier, Second Edition, 2006.

[29] F. Gritti, G. Guiochon, Possible resolution gain in enantioseparations afforded by core-shell particle technology, J. Chromatogr. A 1348 (2014) 87–96.

[30] F. Gritti, G. Guiochon, Mass transfer mechanism in chiral reversed phase liquid chromatography, J. Chromatogr. A 1332 (2014) 35–45.

[31] K. Kaczmarski, A. Cavazzini, P. Szabelski, D. Zhou, X. Liu, G. Guiochon, Application of the general rate model and the generalized Maxwell-Stefan equation to the study of the mass transfer kinetics of a pair of enantiomers, J. Chromatogr. A 962 (2002) 57–67.

[32] A. Felinger, D. M. Zhou, G. Guiochon, Determination of the single component and competitive adsorption isotherms of the 1-indanol enantiomers by the inverse method, J. Chromatogr. A 1005 (2003) 35–49.

[33] M. Catani, R. Guzzinati, N. Marchetti, L. Pasti, A. Cavazzini, Exploring fluorous affinity by liquid chromatography, Anal. Chem. 87 (2015) 6854–6860.

[34] P. Vajda, A. Cavazzini, A. Felinger, Adsorption equilibria of proline in hydrophilic interaction chromatography, J. Chromatogr. A 1217 (2010) 5965–5970.

[35] E. Morgan, K. W. Burton, Optimization using the super-modified simplex method, Chemometr. Intell. Lab. 8 (1990) 97–107.

[36] A. Cavazzini, M. Remelli, F. Dondi, Stochastic theory of two-site adsorption chromatography by the characteristic function method, J. Microcol. Sep. 9 (1997) 295–302.

[37] P. Jandera, V. Bačkovská, A. Felinger, Analysis of the band profiles of the enantiomers of phenylglycine in liquid chromatography on bonded teicoplanin columns using the stochastic theory of chromatography, J. Chromatogr. A 919 (2001) 67–77.

[38] D. Zhou, K. Kaczmarski, A. Cavazzini, X. Liu, G. Guiochon, Modeling of the separation of two enantiomers using a microbore column, J. Chromatogr. A 1020 (2003) 199–217.

[39] A. Cavazzini, F. Dondi, A. Jaulmes, C. Vidal-Madjar, A. Felinger, Monte carlo model of nonlinear chromatography: correspondence between the microscopic stochastic model and the microscopic thomas kinetic model, Anal. Chem. 74 (2002) 6269–6278.

[40] A. Cavazzini, M. Remelli, F. Dondi, A. Felinger, Stochastic theory of multiple-site linear adsorption chromatography, Anal. Chem. 71 (1999) 3453–3462.

[41] T. Fornstedt, P. Sajonz, G. Guiochon, A closer study of chiral retention mechanisms, Chirality 10 (1998) 375–381.

[42] G. Götmar, T. Fornstedt, G. Guiochon, Apparent and true enantioselectivity in enantioseparations, Chirality 12 (2000) 558–564.

[43] G. Götmar, T. Fornstedt, M. Andersson, G. Guiochon, Influence of the solute hydrophobicity on the enantioselective adsorption of beta-blockers on a cellulase protein used as the chiral selector, J. Chromatogr. A 905 (2001) 3–17.

[44] F. Gritti, G. Guiochon, Critical contribution of nonlinear chromatography to the understanding of retention mechanism in reversed-phase liquid chromatography, J. Chromatogr. A 1099 (2005) 1–42.

[45] A. Cavazzini, K. Kaczmarski, P. Szabełski, D. M. Zhou, X. D. Liu, G. Guiochon, Modeling of the separation of the enantiomers of 1-phenyl-1-propanol on cellulose tribenzoate, Anal. Chem. 73 (2001) 5704–5715.

[46] N. Marchetti, L. Caciolli, A. Laganà, F. Gasparrini, L. Pasti, F. Dondi, A. Cavazzini, Fluorous affinity chromatography for enrichment and determination of perfluoroalkyl substances, Anal. Chem. 84 (2012) 7138–7145.

[47] A. Cavazzini, N. Marchetti, R. Guzzinati, L. Pasti, A. Ciogli, F. Gasparrini, A. Laganá, Understanding mixed-mode retention mechanisms in liquid chromatography with hydrophobic stationary phases, Anal. Chem. 86 (2014) 4919–4926.

[48] F. Gritti, Y. V. Kazakevich, G. Guiochon, Effect of the surface coverage of endcapped C_{18}-silica on the excess adsorption isotherms of commonly used organic solvents from water in reversed phase liquid chromatography, J. Chromatogr. A 1169 (2007) 111–124.

[49] S. Bocian, P. Vajda, A. Felinger, B. Buszewski, Solvent excess adsorption on the stationary phases for reversed-phase liquid chromatography with polar functional groups, J. Chromatogr. A 1204 (2007) 35–41.

[50] K. Balmér, P. O. Lagerström, B. A. Persson, G. Schill, Reversed retention order and other stereoselective effects in the separation of amino alcohols on Chiralcel OD, J. Chromatogr. 592 (1992) 331–337.

[51] S. Ma, S. Shen, H. Lee, M. Eriksson, X. Zeng, J. Xu, K. Fandrick, N. Yee, C. Senanayake, N. Grinberg, Mechanistic studies on the chiral recognition of polysaccharide-based chiral stationary phases using liquid chromatography and vibrational circular dichroism: Reversal of elution order of N-substituted alpha-methyl phenylalanine esters, J. Chromatogr. A 1216 (2009) 3784–3793.

[52] L. Chankvetadze, N. Ghibradze, M. Karchkhadze, L. Peng, T. Farkas, B. Chankvetadze, Enantiomer elution order reversal of fluorenylmethoxycarbonyl-isoleucine in high-performance liquid chromatography by changing the mobile phase temperature and composition, J. Chromatogr. A 1218 (2011) 6554–6560.

[53] R. Guzzinati, E. Sarti, M. Catani, V. Costa, A. Pagnoni, A. Martucci, E. Rodeghero, D. Capitani, M. Pietrantonio, A. Cavazzini, L. Pasti, Formation of supramolecular clusters at the interface of Zeolite X following the adsorption of rare-earth cations and their impact on the macroscopic properties of the Zeolite, ChemPhysChem (2018) DOI: 10.1002/cphc.201800333.

Figure 1

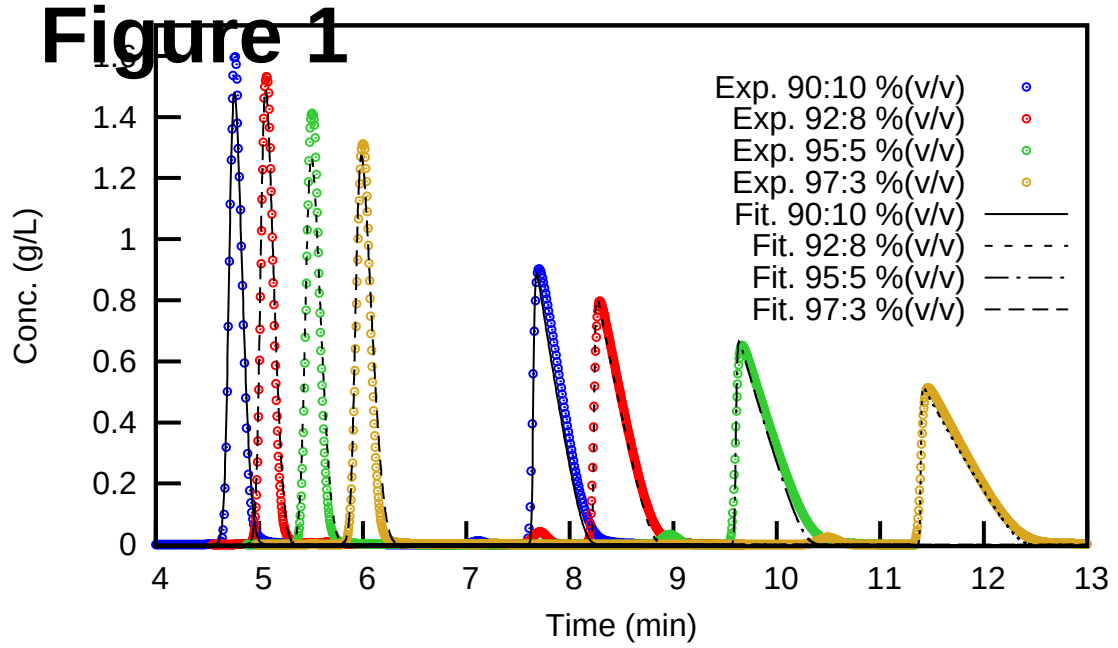
Exp. 90:10 %(v/v)
Exp. 92:8 %(v/v)
Exp. 95:5 %(v/v)
Exp. 97:3 %(v/v)
Fit. 90:10 %(v/v)
Fit. 92:8 %(v/v)
Fit. 95:5 %(v/v)
Fit. 97:3 %(v/v)
Conc. (g/L)
Time (min)

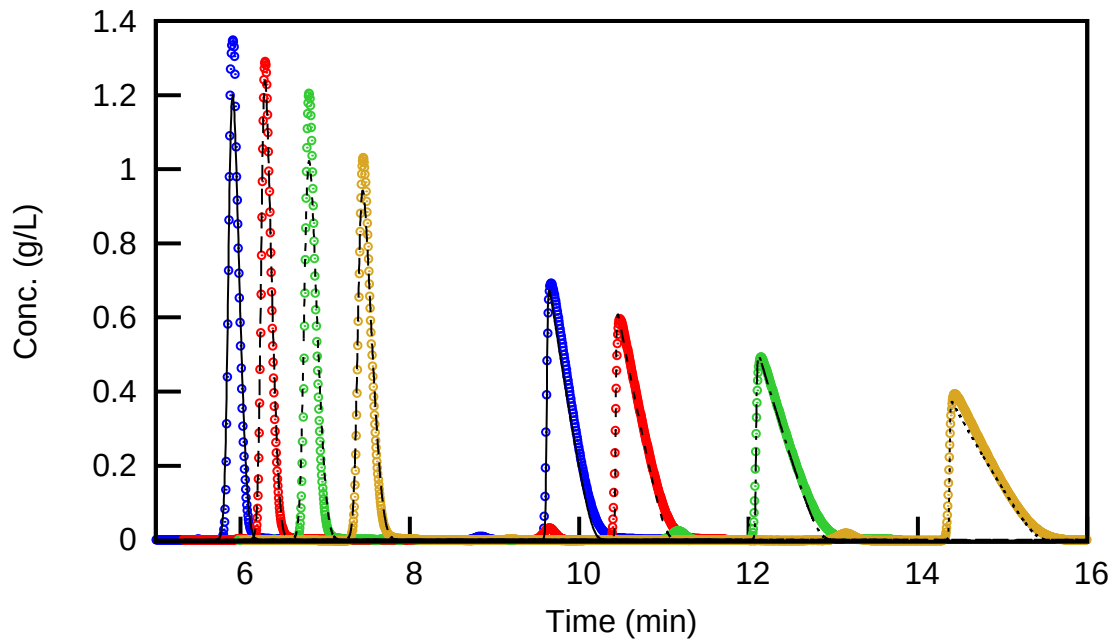
Conc. (g/L)
Time (min)

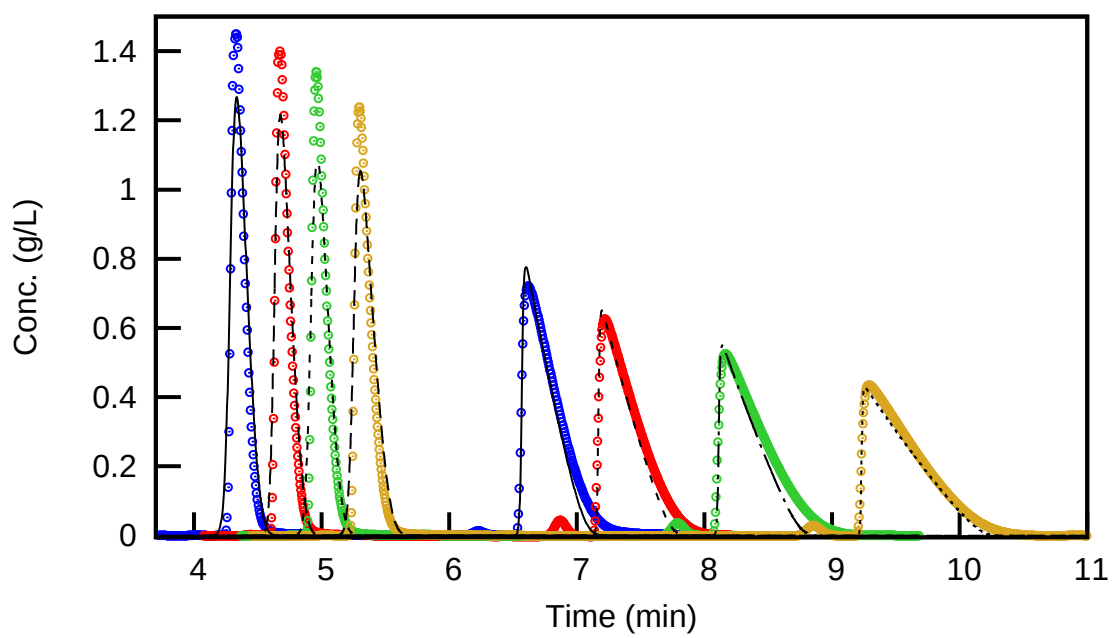
Conc. (g/L)
Time (min)

Figure 2

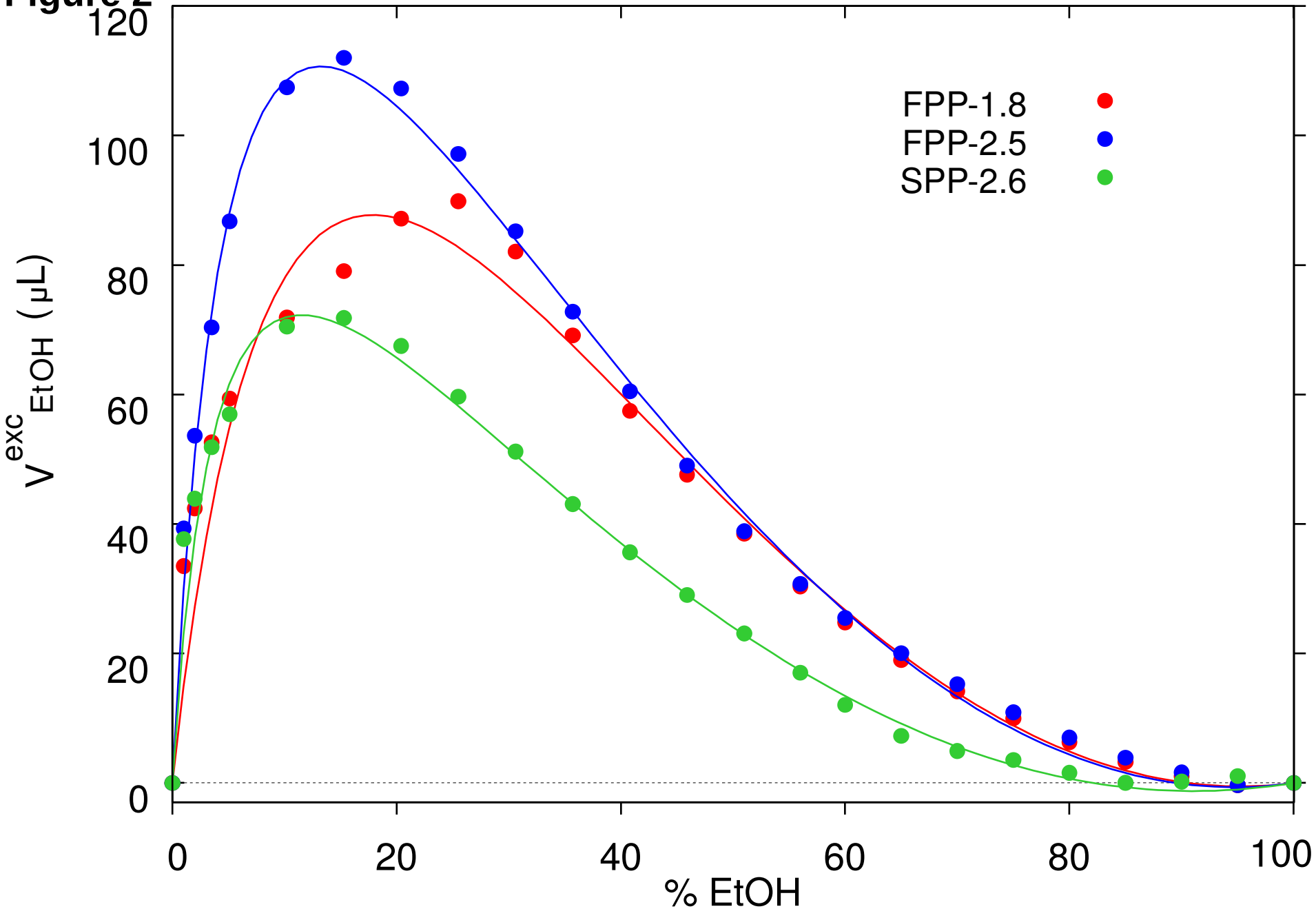

Figure 3

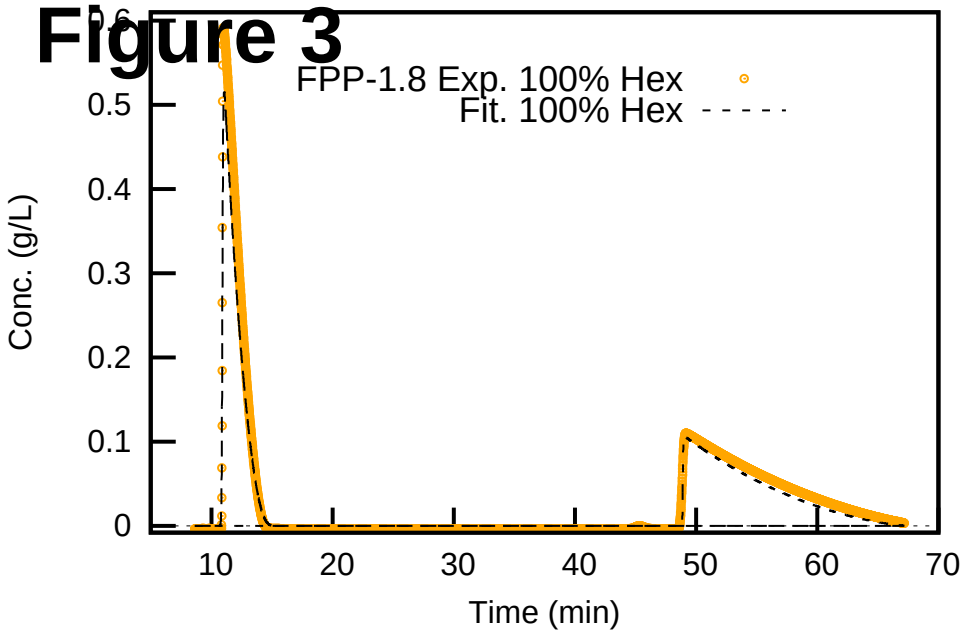
FPP-1.8 Exp. 100% Hex
Fit. 100% Hex
Conc. (g/L)
Time (min)
0
0.1
0.2
0.3
0.4
0.5
0.6
10
20
30
40
50
60
70

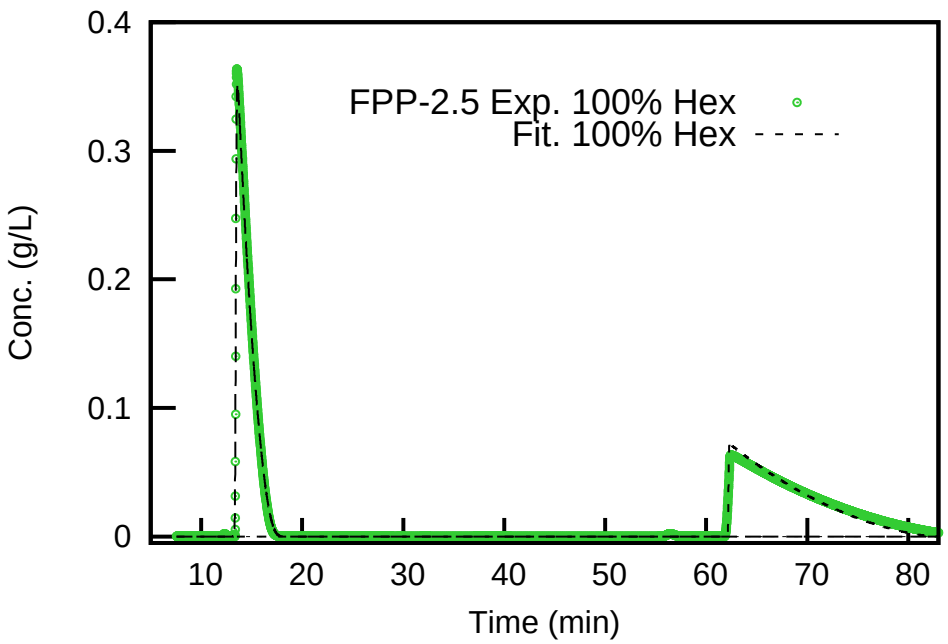
FPP-2.5 Exp. 100% Hex
Fit. 100% Hex
Conc. (g/L)
Time (min)
0
0.1
0.2
0.3
0.4
10
20
30
40
50
60
70
80

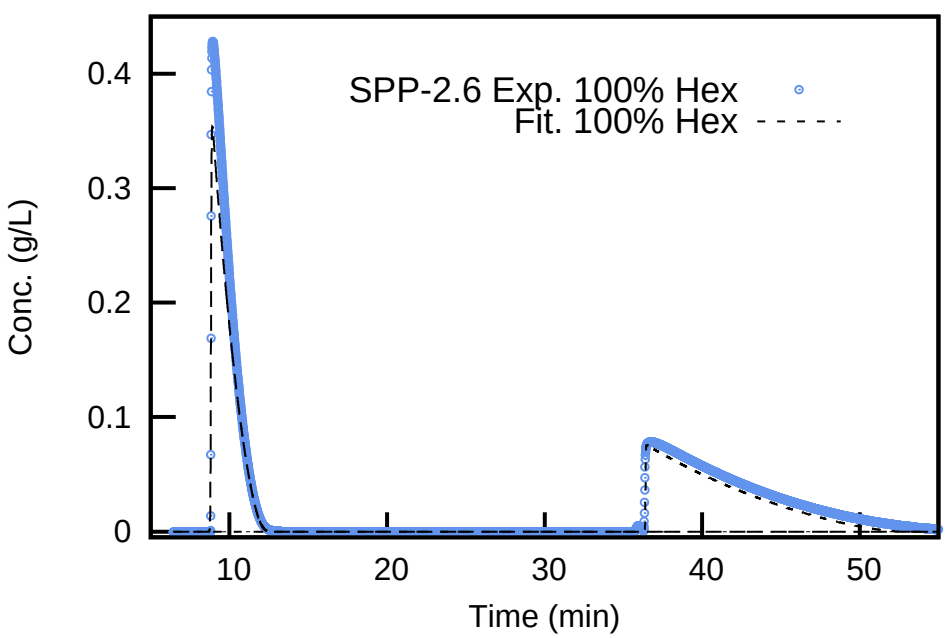
SPP-2.6 Exp. 100% Hex
Fit. 100% Hex
Conc. (g/L)
Time (min)
0
0.1
0.2
0.3
0.4
10
20
30
40
50

Electronic Supplementary Material (online publication only)

Click here to download Electronic Supplementary Material (online publication only): suppl_material.pdf

LaTeX Source Files

Click here to download LaTeX Source Files: LaTex_source_paper_revised_R1.zip